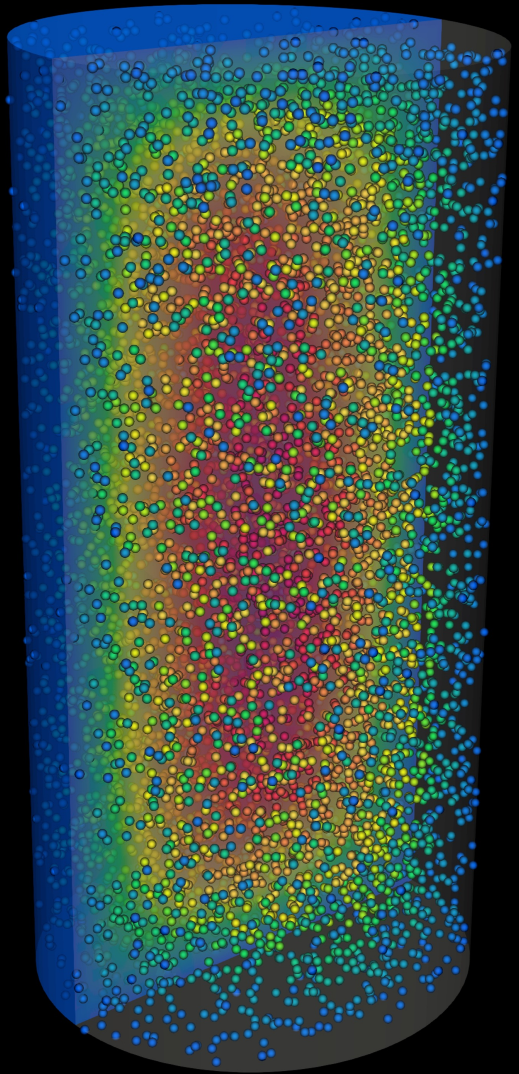

Bison

2021 R&D 100 WINNER

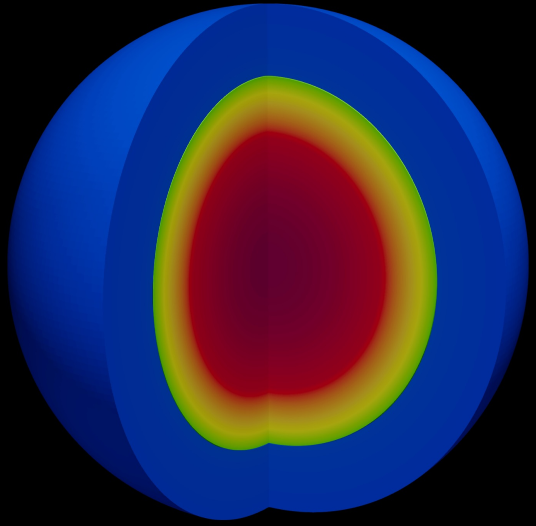

Oct 20, 2022

TRISO PARTICLE FUEL PERFORMANCE WITH BISON

Wen Jiang, Presented by Pierre-Clément Simon

Idaho National Laboratory

INL/CON-22-69598

Multi-scale TRISO modeling overview

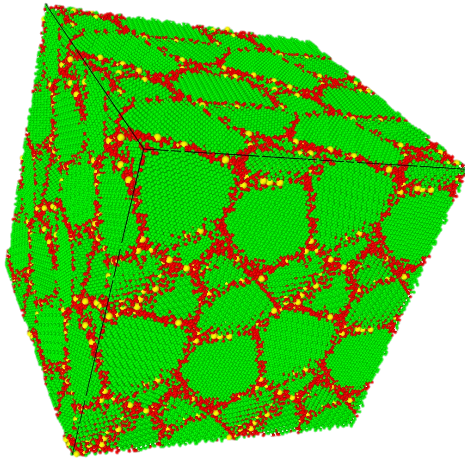

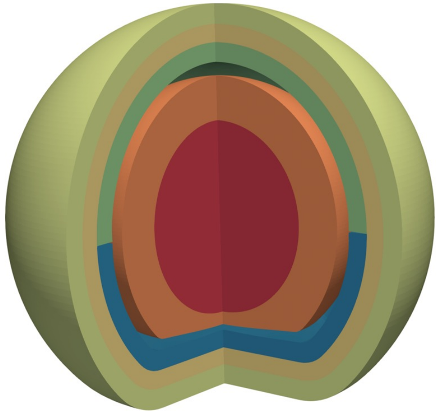

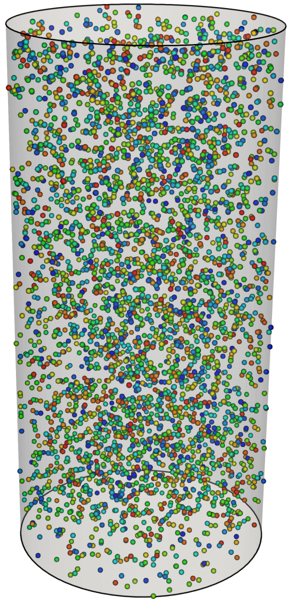

Lower-length scale modeling

- **Fission gas release model:** Xe, Kr diffusivity in UCO
- **Fission product diffusivity:** Silver diffusion in SiC, Pd Penetration

TRISO particle

- **Thermal-mechanical modeling**
  - **Failure analysis:** asphericity, IPyC cracking and debonding
- **Fission product diffusion through layers**

Pebble and Compact modeling

- **Failure probability calculation**: Monte Carlo and Fast Integration Approach
- **Fission product diffusion through matrix**
- **Particle-Matrix interaction**

TRISO Fuel Particle Modeling

Kernel
Thermal
Burnup
Elasticity Tensor
Volumetric Swelling
Fission Gas Release

Buffer
Thermal
Elasticity Tensor
Creep
Thermal Expansion
IIDC

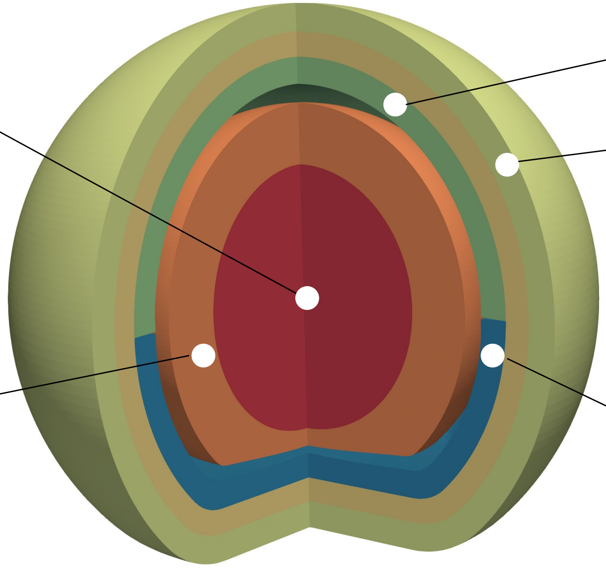

IPyC and OPyC
Thermal Expansion
Elasticity Tensor
Creep
IIDC

SiC
Elasticity Tensor
Thermal Expansion

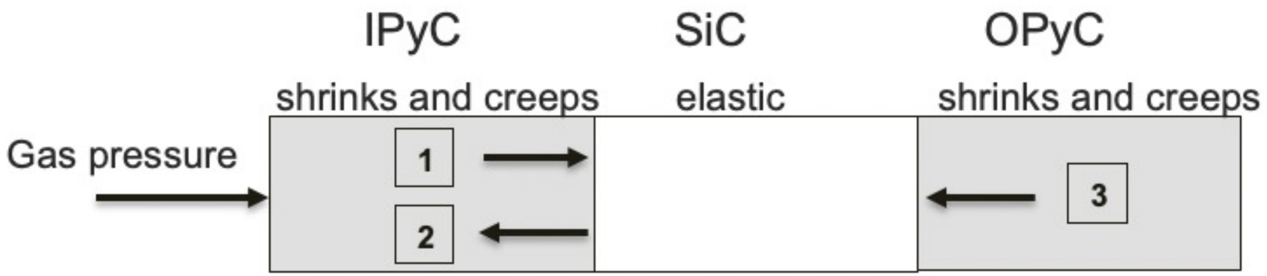

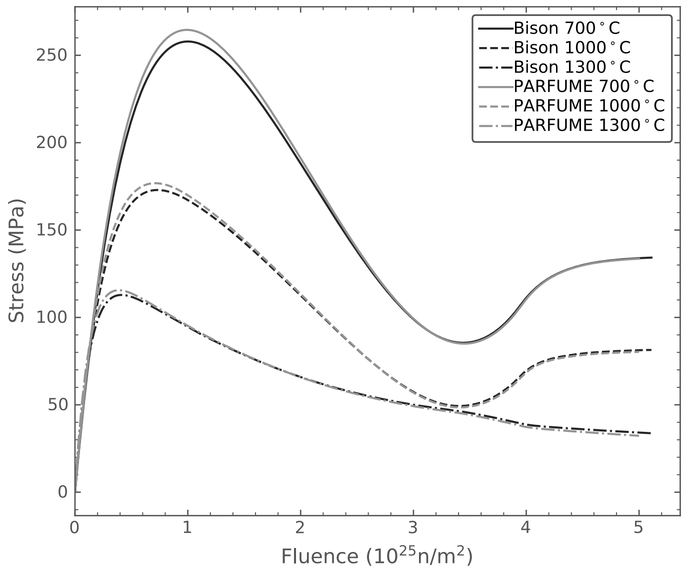

Tangential stress in IPyC

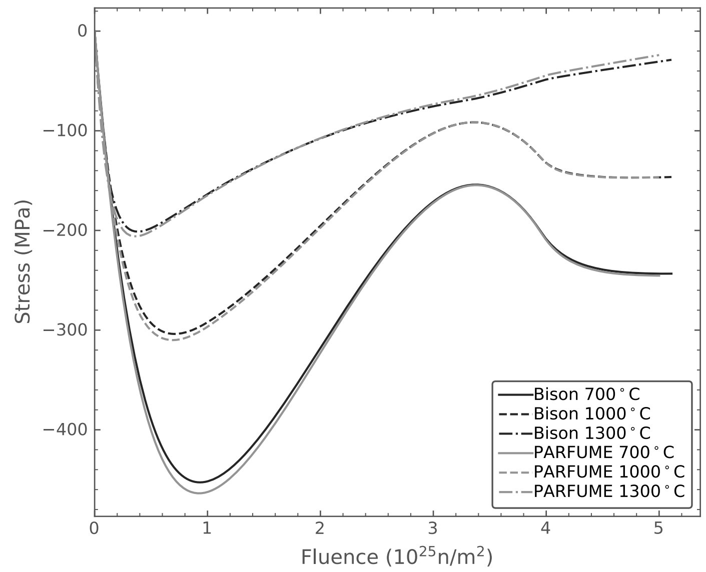

Tangential stress in SiC

TRISO Failure Modes

- **Mechanical**
  - Pressure vessel failure
  - Irradiation-induced PyC failure leading to SiC cracking
  - IPyC-SiC / Buffer-IPyC partial debonding

- **Thermochemical**
  - Kernel migration
  - SiC thermal decomposition
  - Fission product attack of SiC
  - Corrosion of SiC by CO

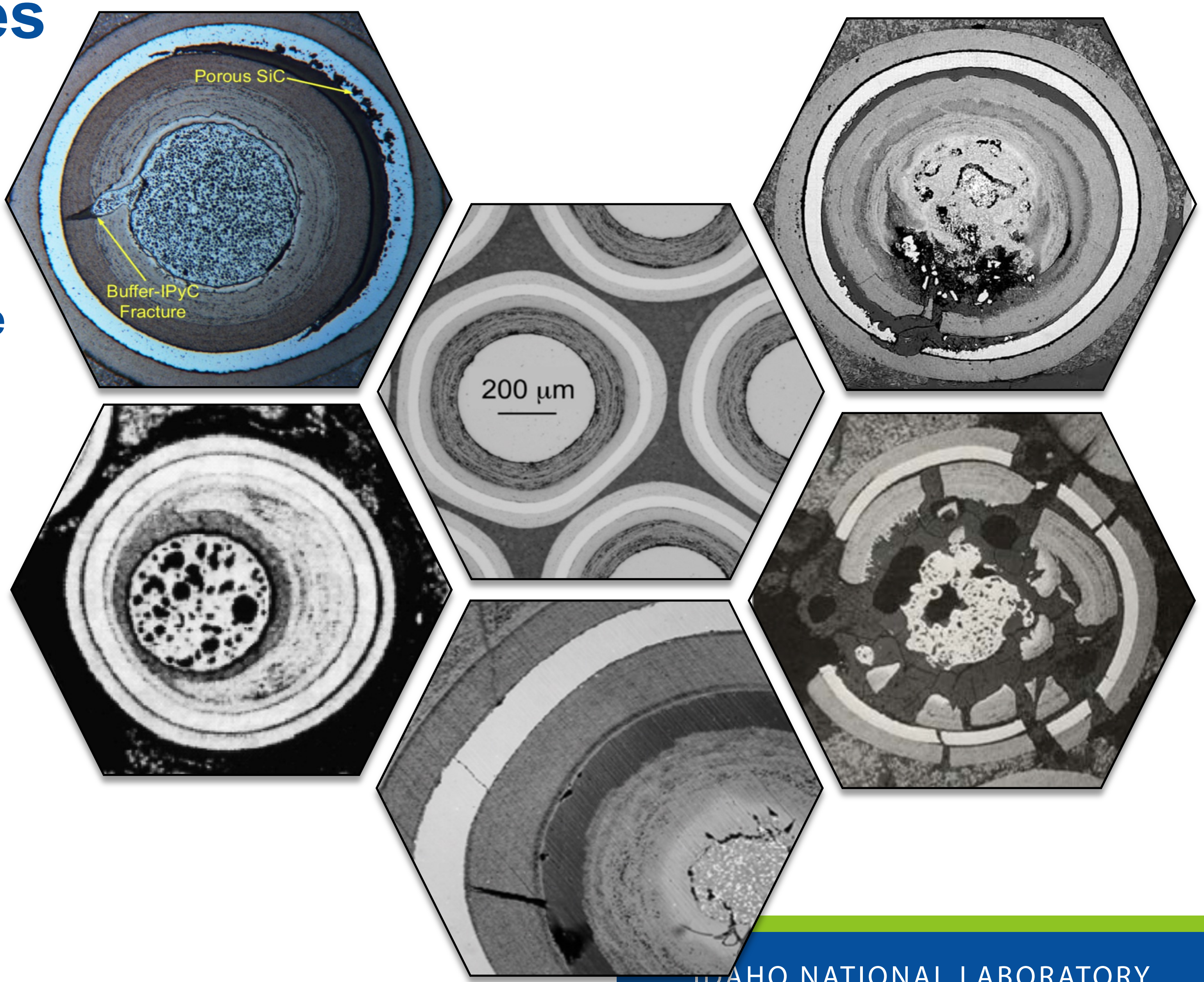

IPyC Cracking

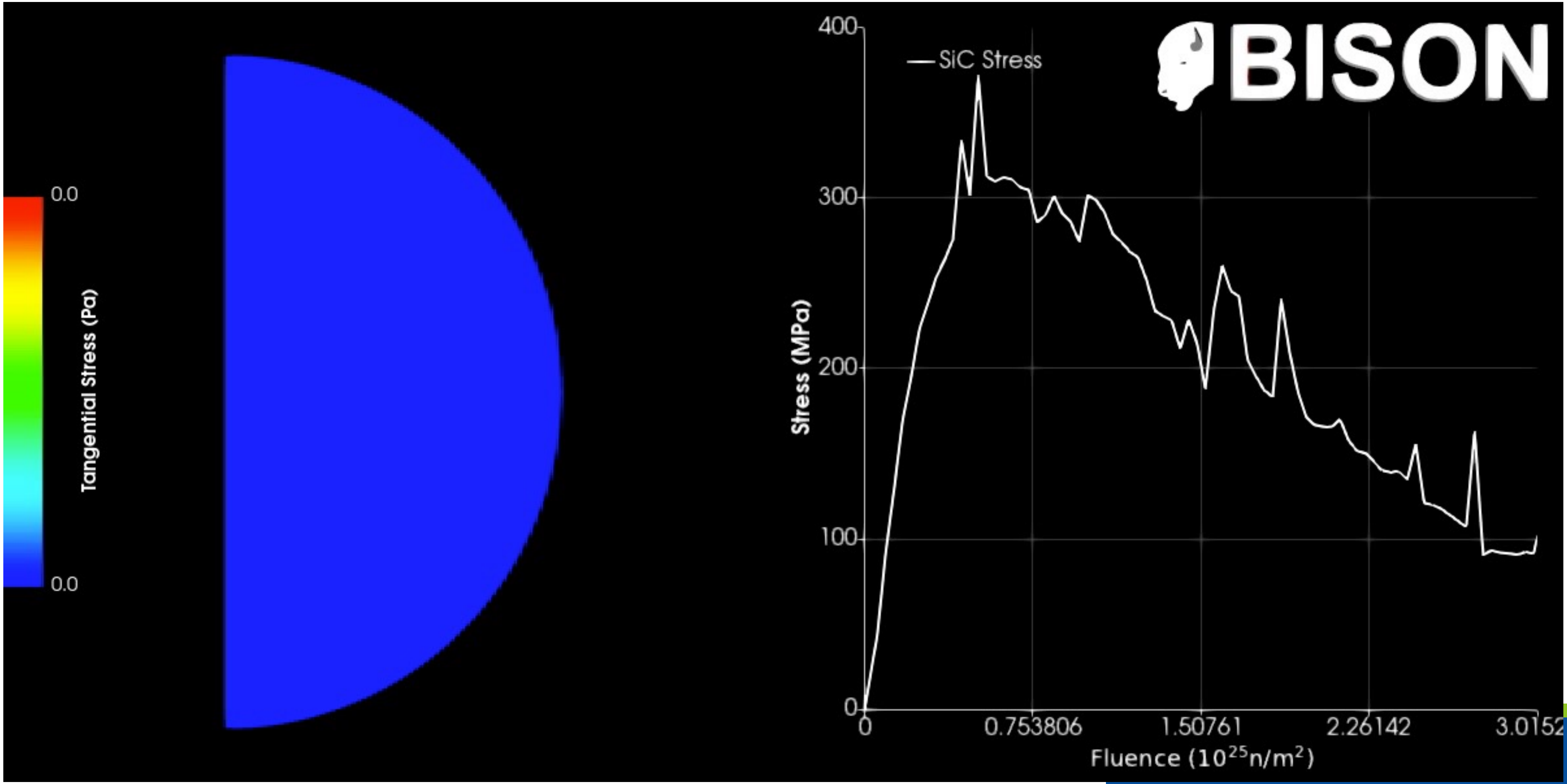

Aspherical particle

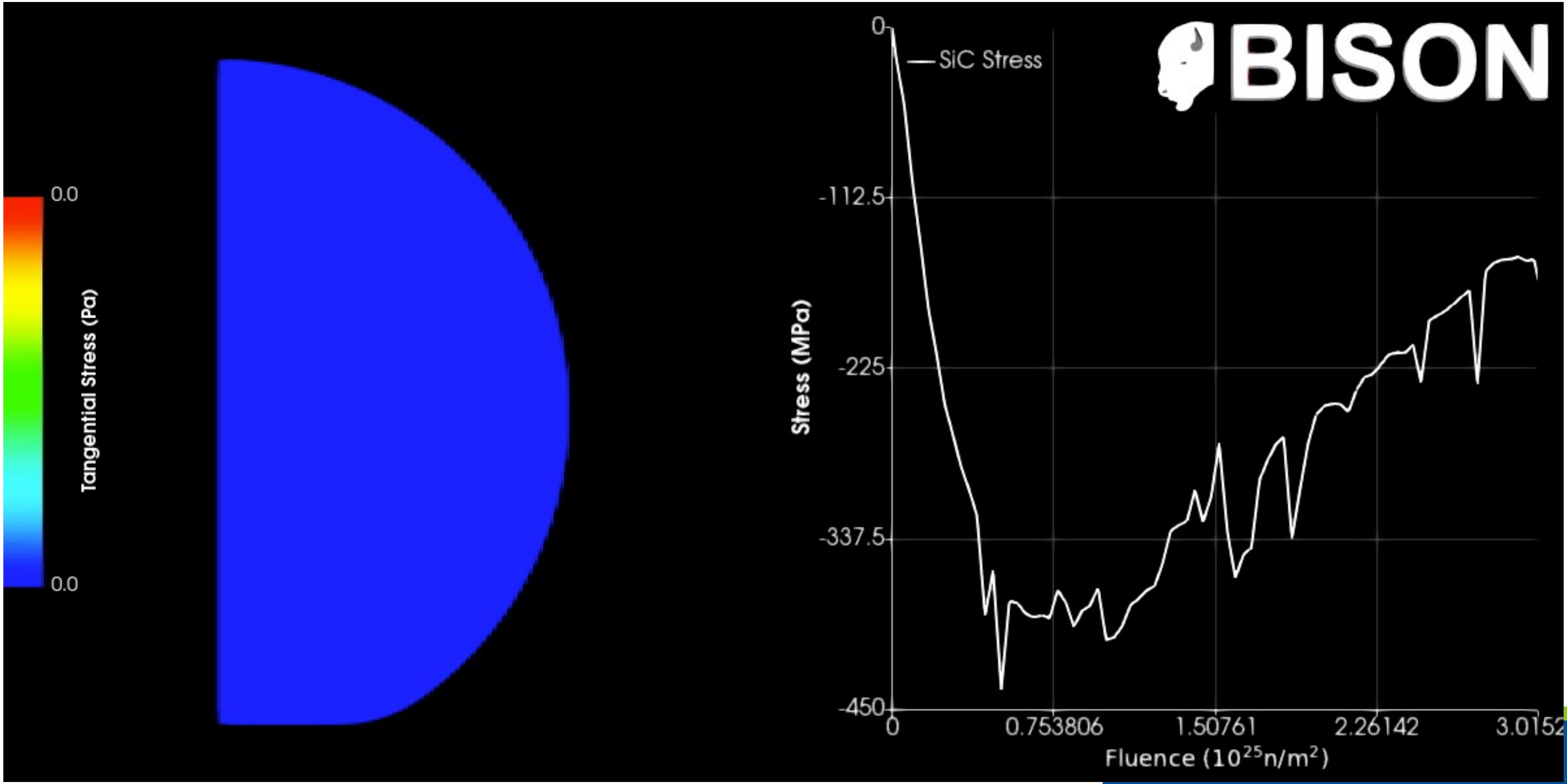

Debonding/tearing with cohesive-zone method

- Partial debonding between the IPyC and the SiC has also been observed in PIE of the NP-MHTGR fuel particles.
- During irradiation, shrinkage of the IPyC layer induces a radial tensile stress at the interface between the IPyC and SiC layer.
- If the stress exceeds the bond strength between layers, then debonding of the IPyC from the SiC occurs.
- A stress concentration occurs in the SiC layer at the tip of the debonded region, containing tensile stress components that could contribute to failure of the SiC.

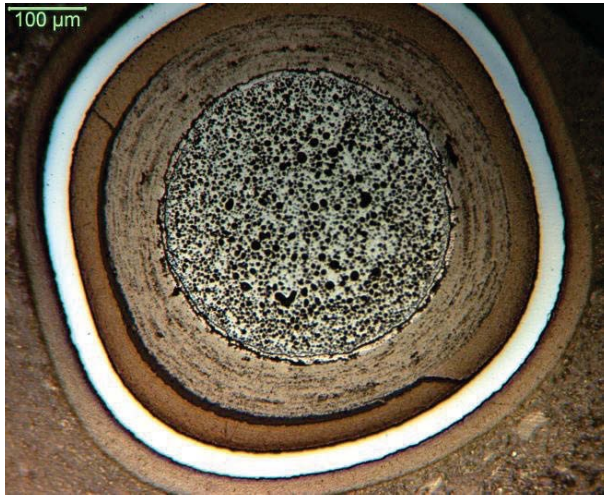

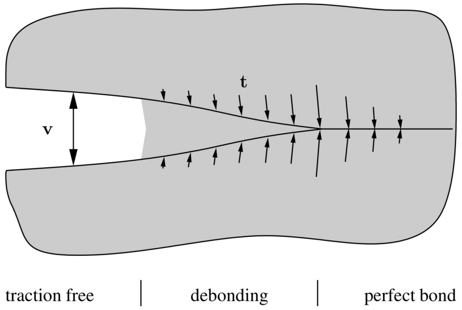

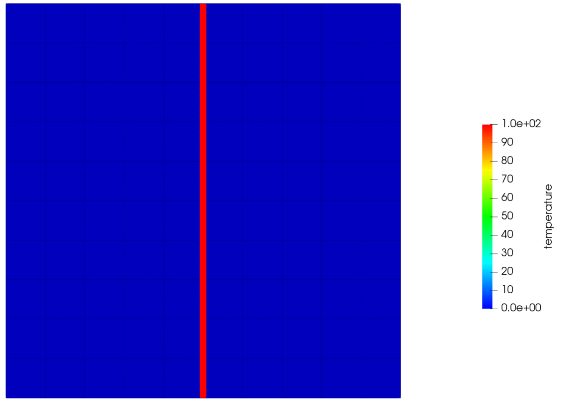

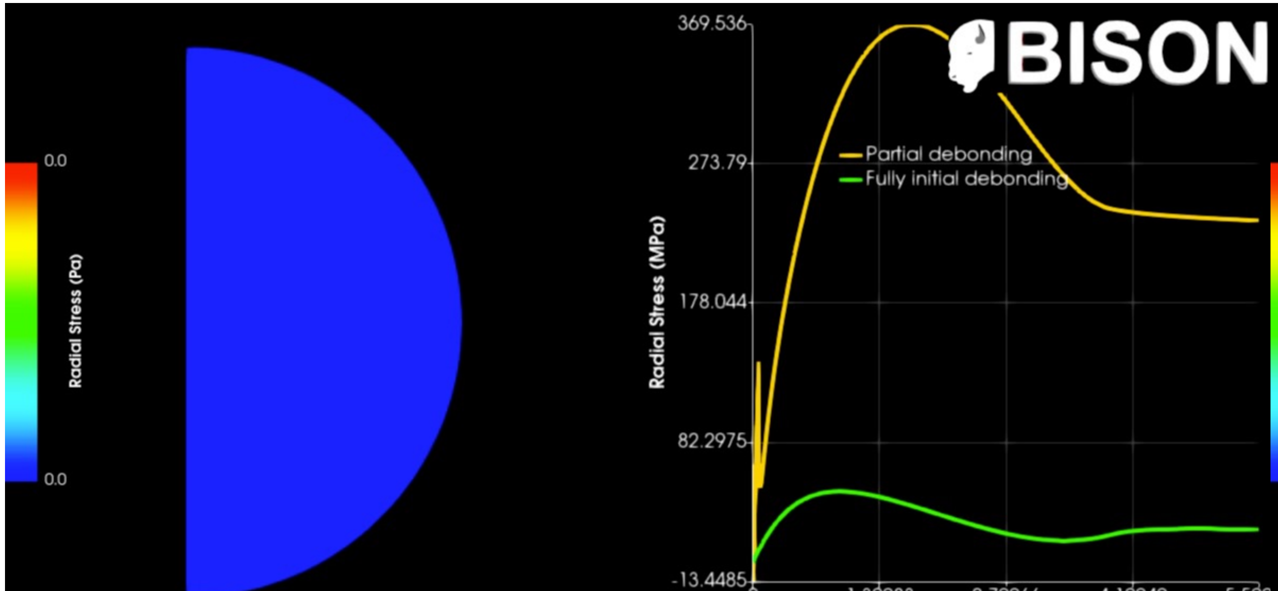

Partial debonding of the buffer from the IPyC

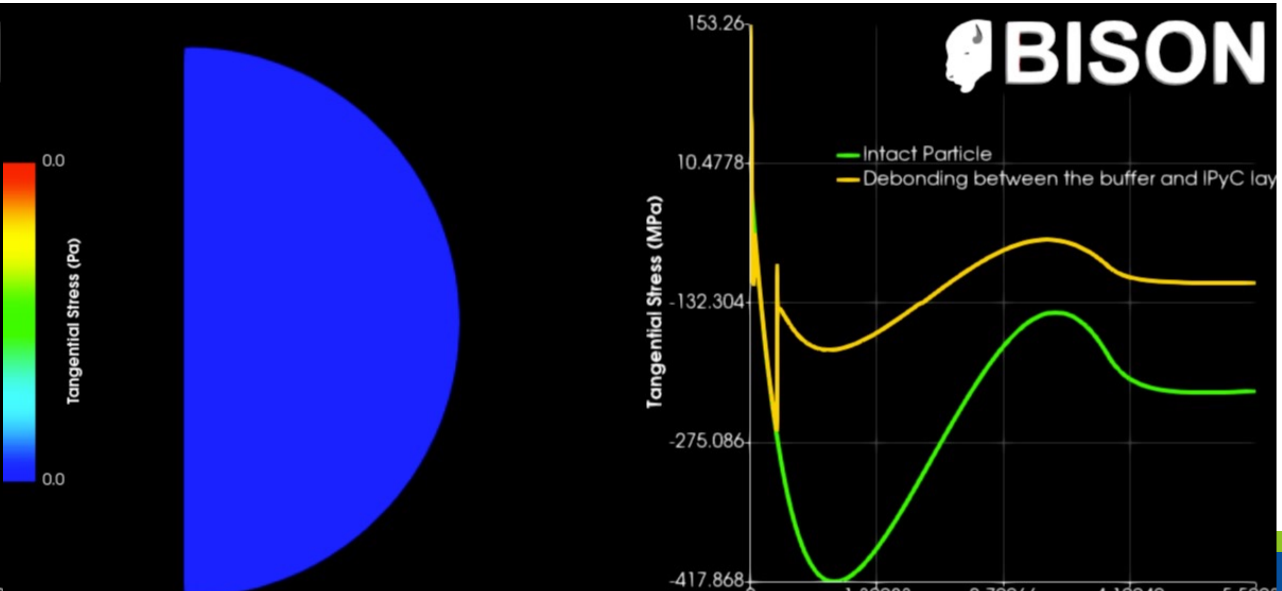

Debonding of the buffer from the IPyC and the IPyC from the SiC layer

Fission Product Diffusion

Conservation of fission product species:

$$\frac{\partial C}{\partial t} + \nabla \cdot \boldsymbol{J} + \lambda C - p = 0$$

Mass flux:

$$\boldsymbol{J} = -\mathrm{D}\nabla C$$

Diffusion Coeffient:

$$\mathrm{D} = \sum_i D_{0,i} \exp(\frac{-Q_i}{RT})$$

Mass passed outside the particle:

$$r = \int\int -D\nabla C \cdot n \; dt \; dA$$

Total fission product production:

$$p = \int\int \Gamma \dot{F} \; dt \; dV$$

Release fraction:

$$f = \frac{r}{p}$$

Verification problems:

- In-pile condition for a short-lived FP
- In-pile condition for a long-lived FP
- Out-of-pile condition
- Evaporation from the outer surface, for both short- and long-lived FPs

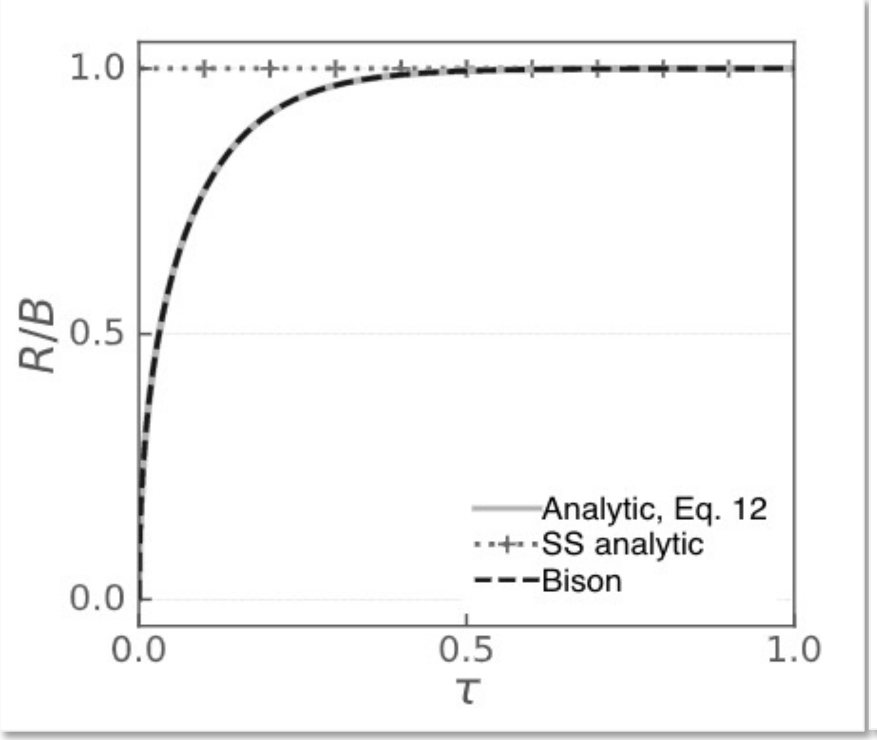

Release rate over birth-rate (R/B)

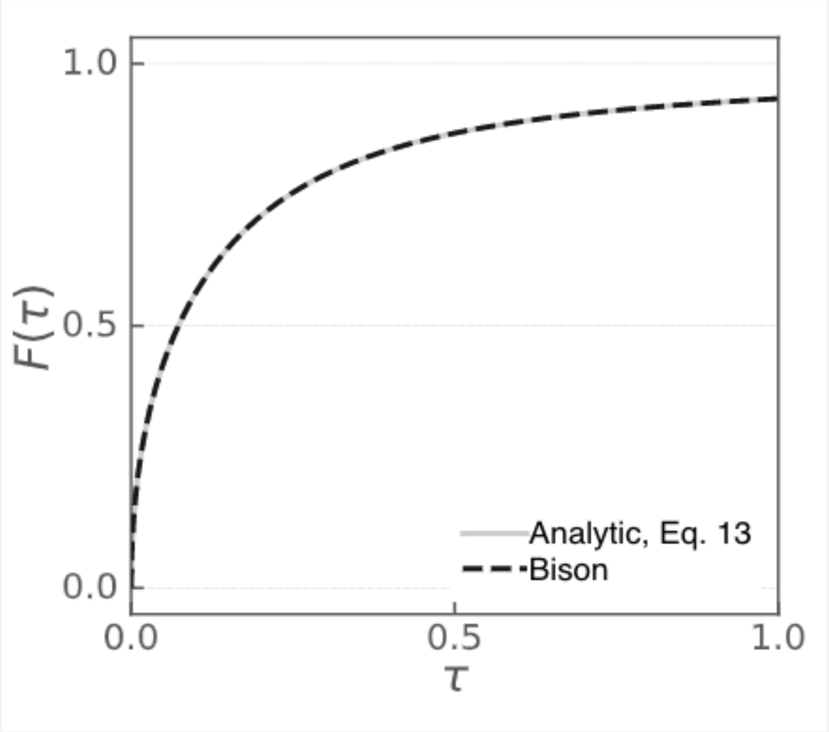

Release fraction

Fission product diffusion through intact and failed particle

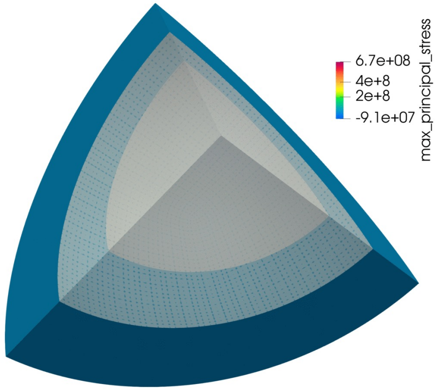

Intact Particle

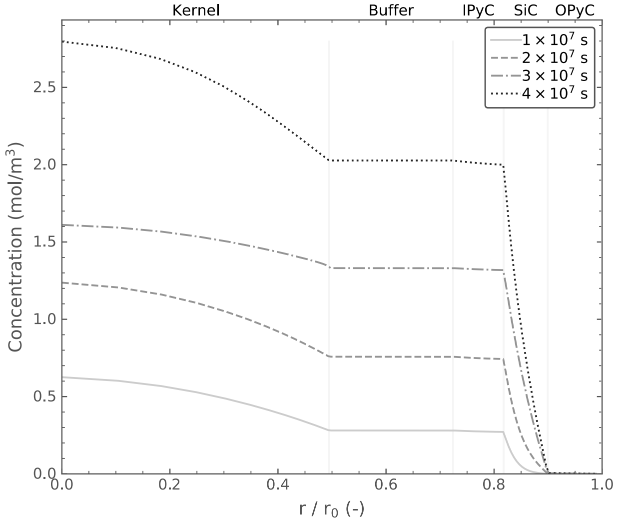

Silver

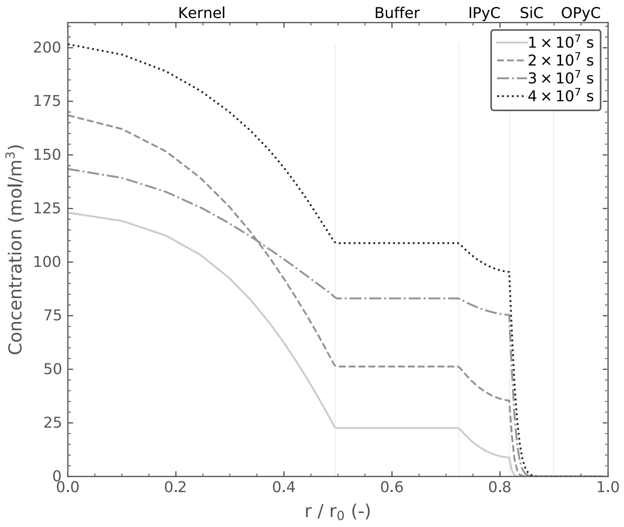

Cesium

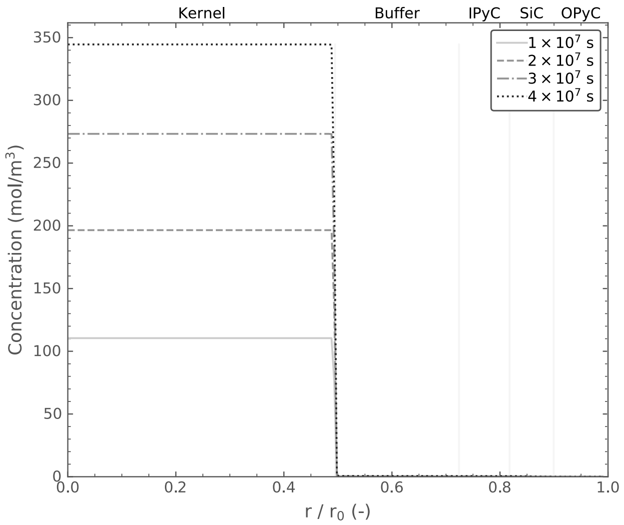

Strontium

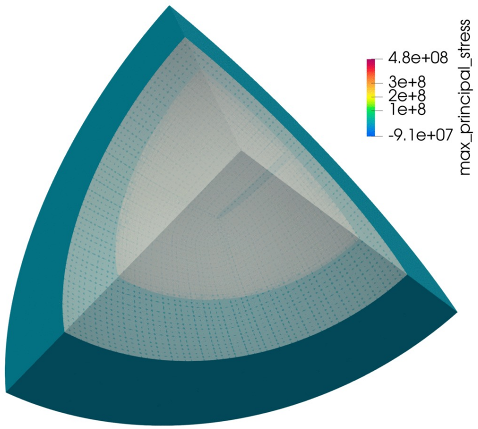

Failed Particle

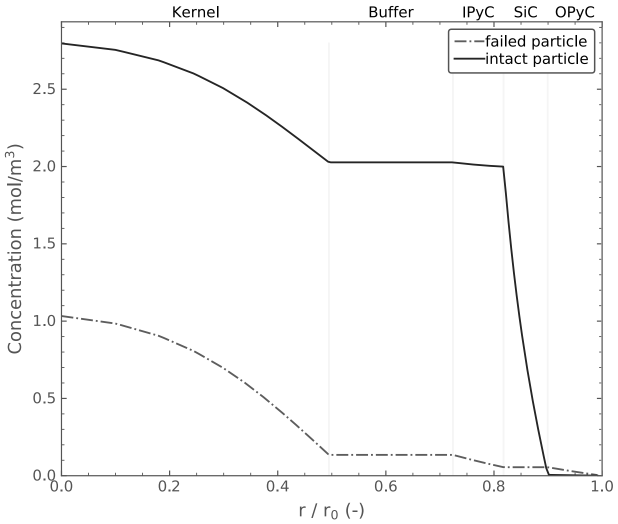

Silver

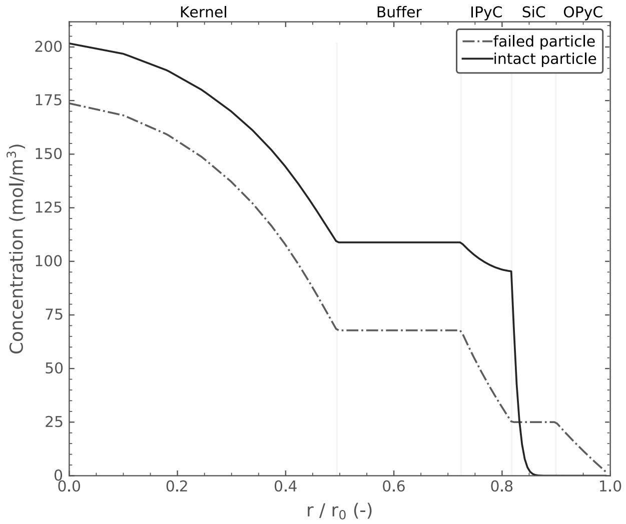

Cesium

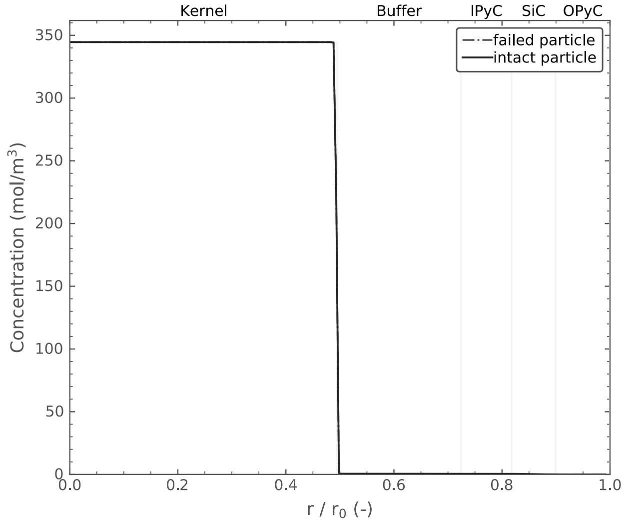

Strontium

AGR-2 Validation

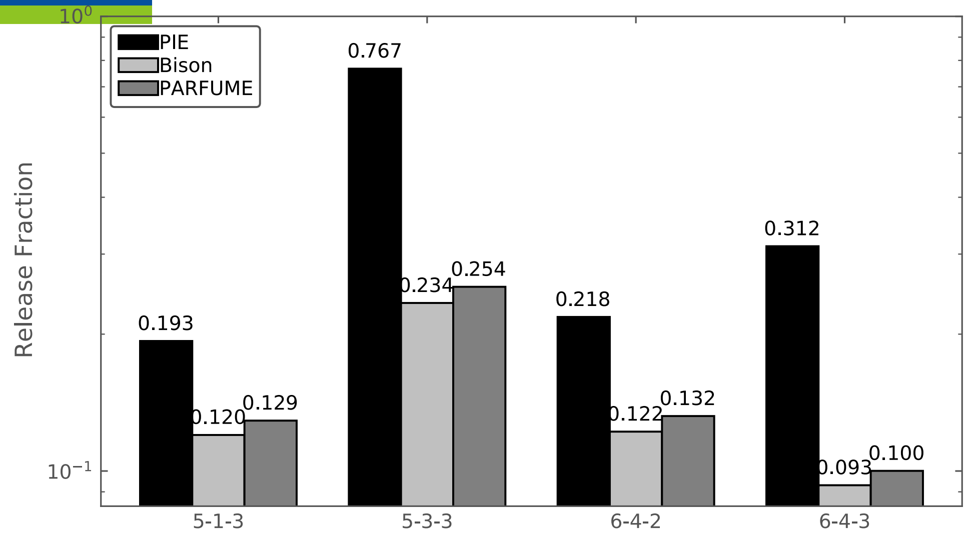

Silver release fractions

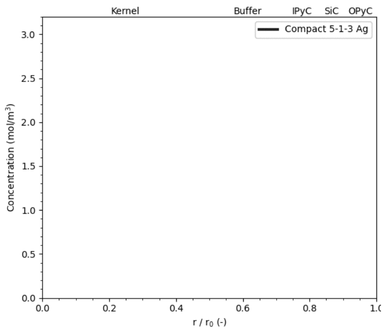

Silver compact 5-1-3

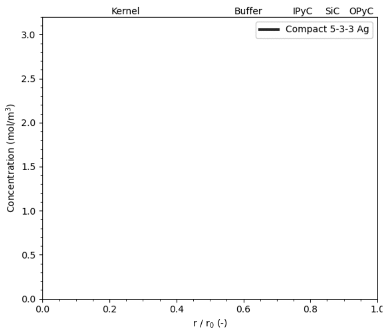

Silver compact 5-3-3

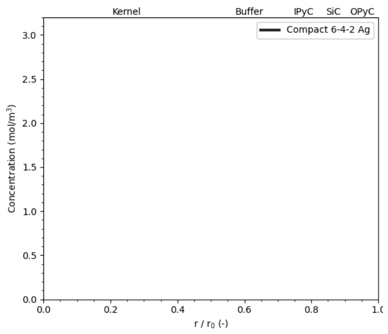

Silver compact 6-4-2

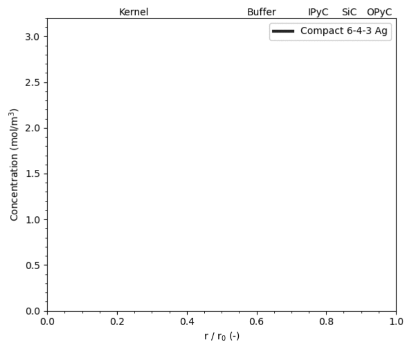

Silver compact 6-4-3

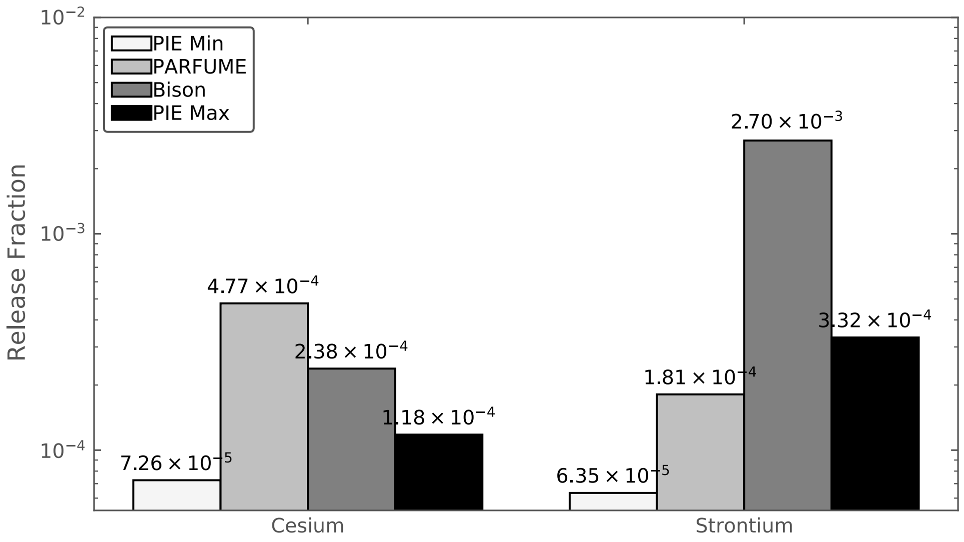

Cesium and Strontium release fractions (Compact 5-3-3)

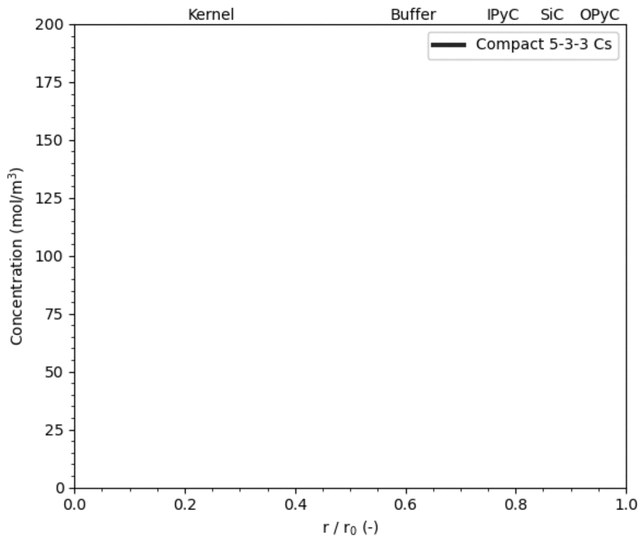

Cesium compact 5-3-3

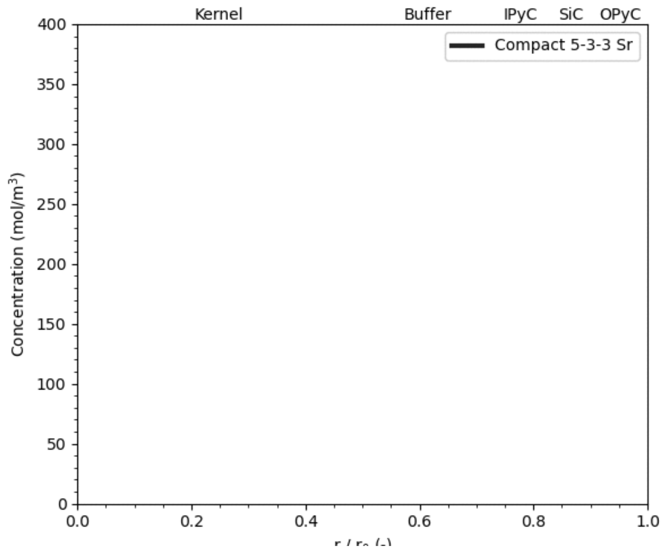

Strontium compact 5-3-3

Fuel elements modeling

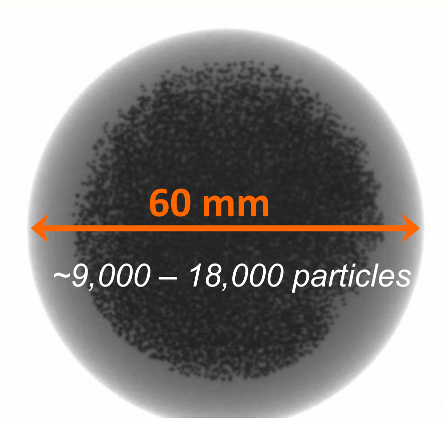

Spherical fuel elements

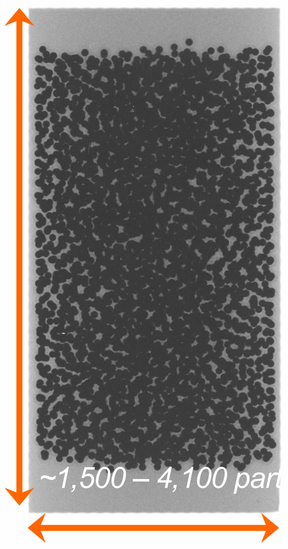

Cylindrical fuel elements

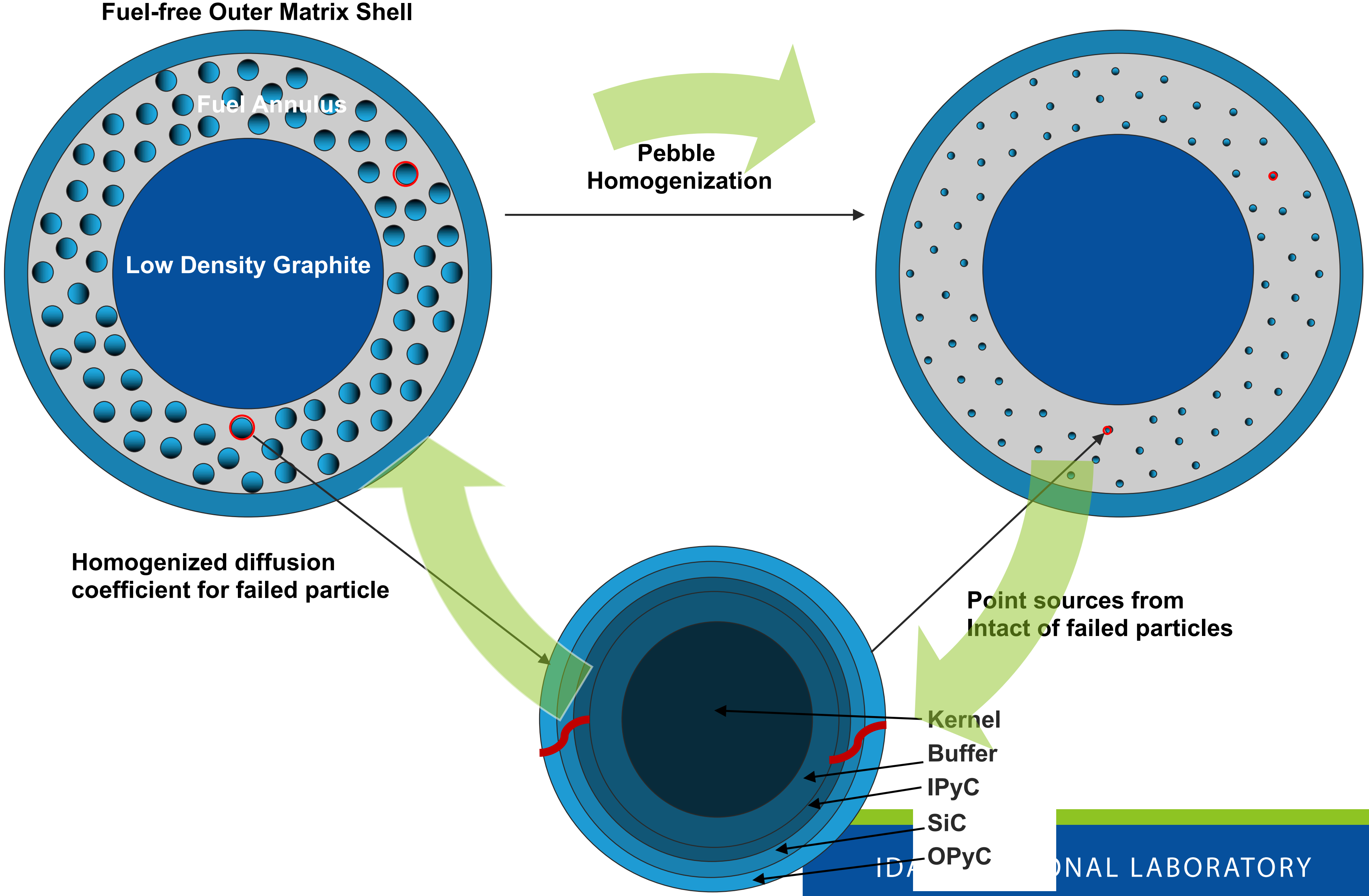

Two-way coupling between particles and matrix

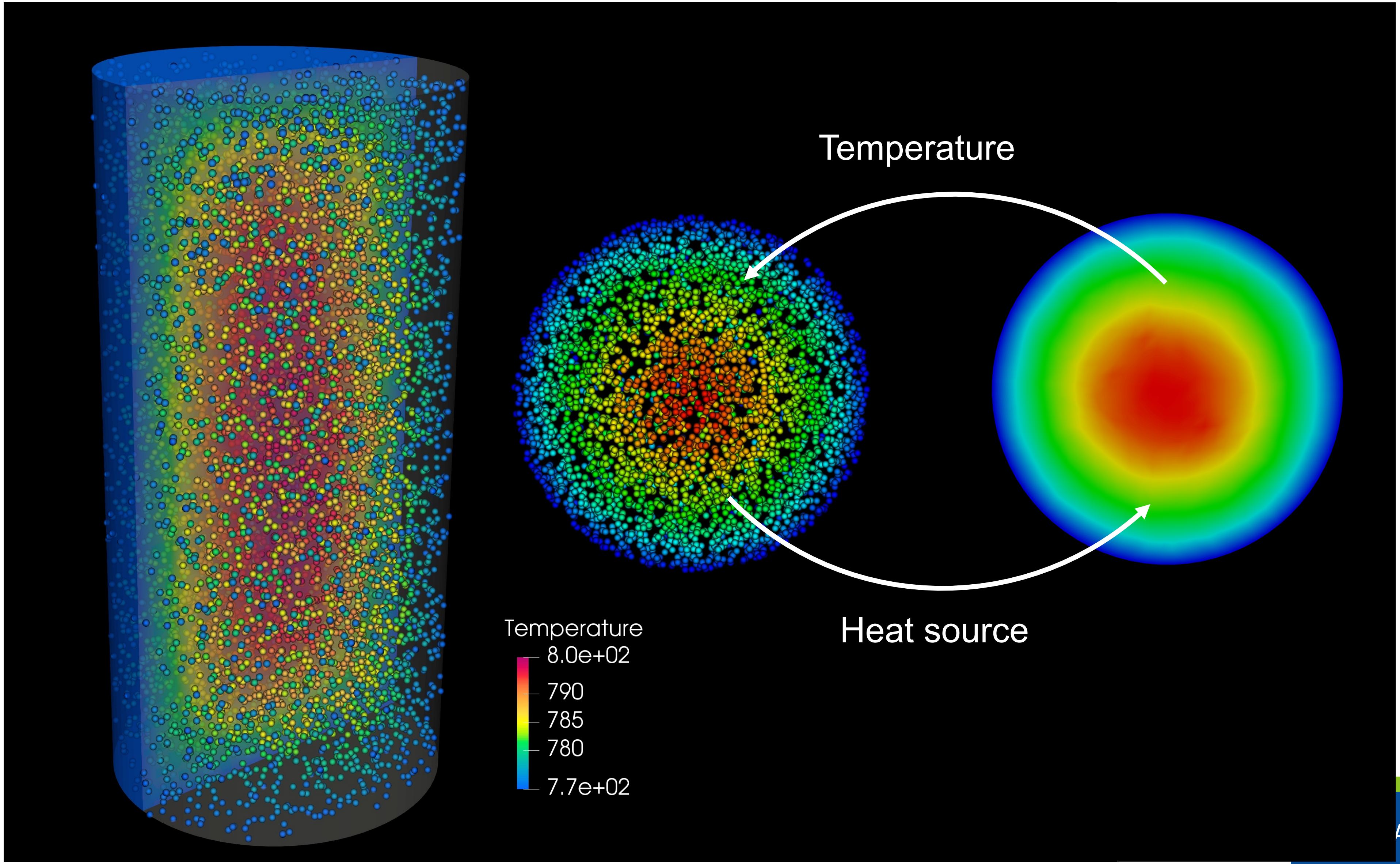

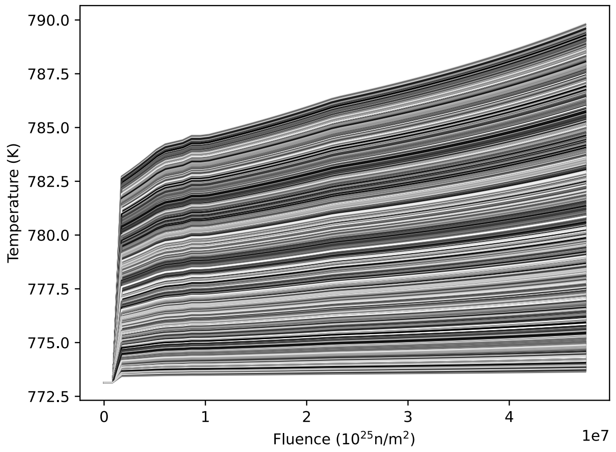

Exterior temp of all particles

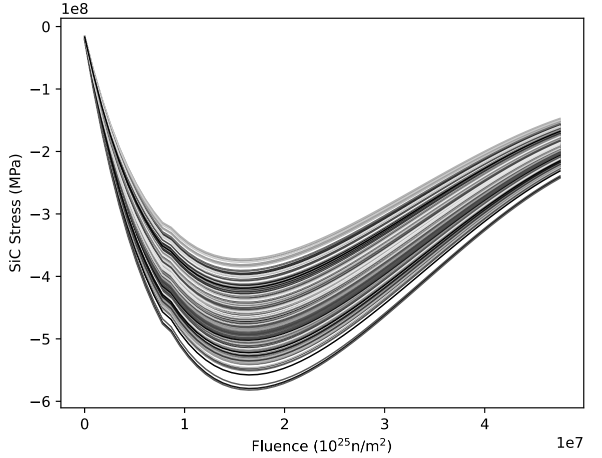

SiC stress of all particles

Pebble modeling

RADIUS (CM)	2.000
SHELL LAYER THICKNESS (CM)	0.200
FUEL LAYER THICKNESS (CM)	0.420
(AGR-5/6/7) TRISOS	9022
U-235 ENRICHMENT (% WT)	19.55

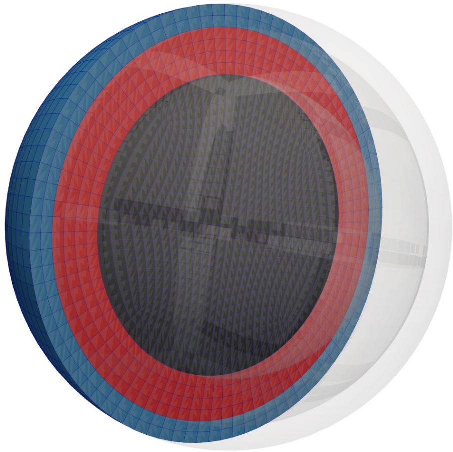

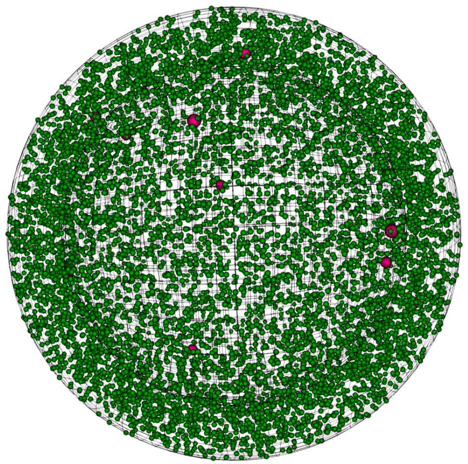

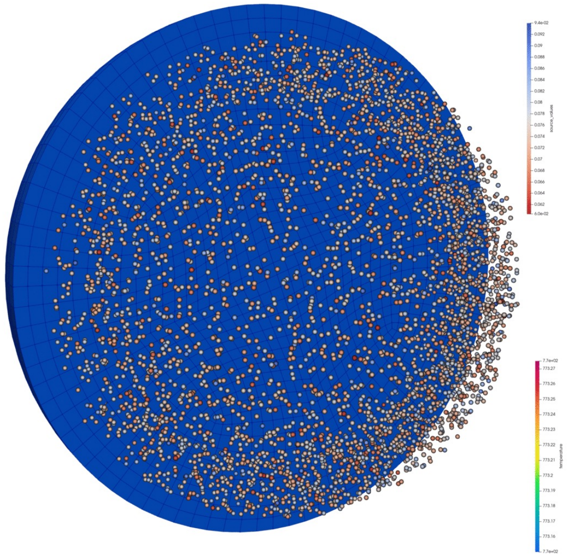

Heat point source

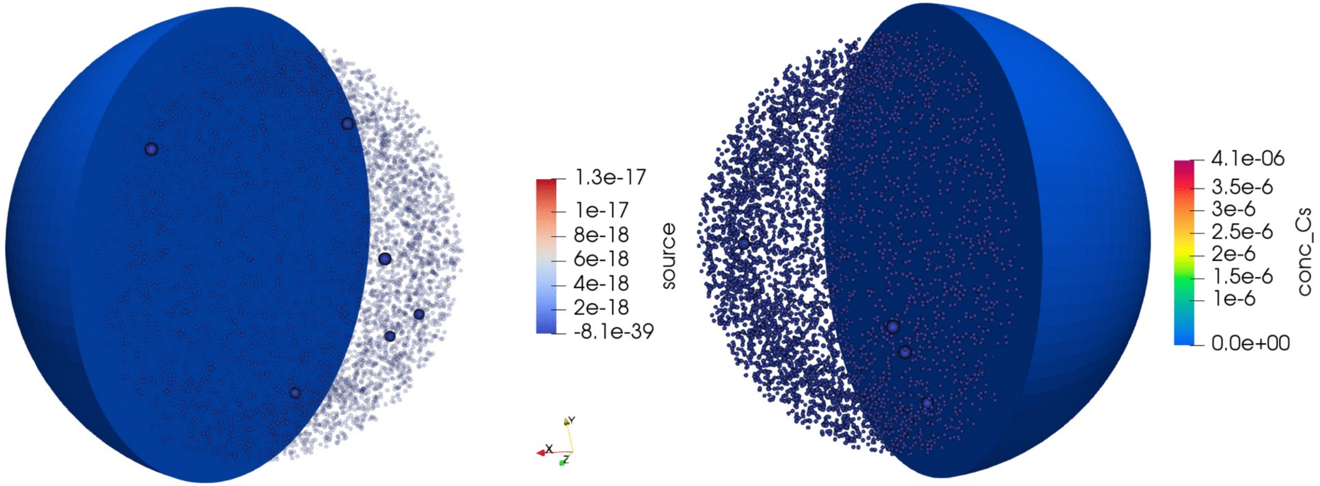

Cs point source

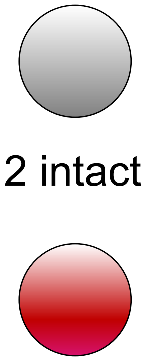

9012 intact particles

10 failed particles

Graphite Matrix Modeling

- **The cores and reflectors in HTGRs are made of graphite materials**
  - the graphite acting as a moderator, a fuel host matrix, a structural component to provide
    - channels for fuel, coolant gas, and control rods
    - a thermal/neutron shielding component
    - heat sink/conduction path during transients

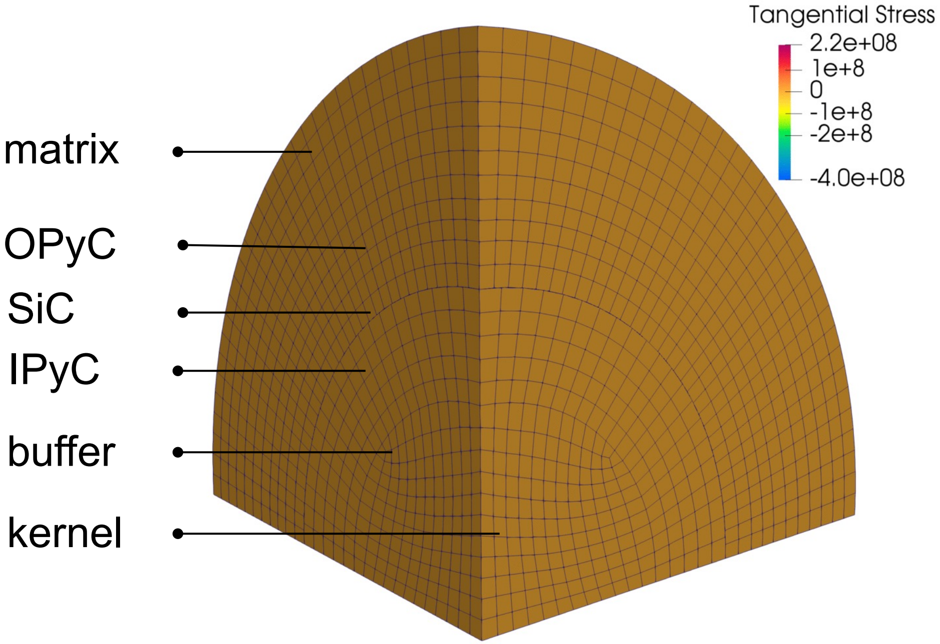

Tangential stress during irradiation for the particle-matrix debonding example (displacements are magnified 2x)

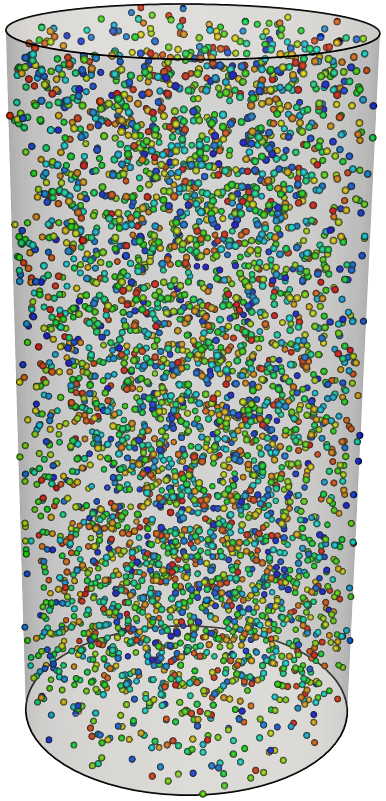

Fuel compact containing 4,000 TRISO particles randomly generated from an MC simulation.

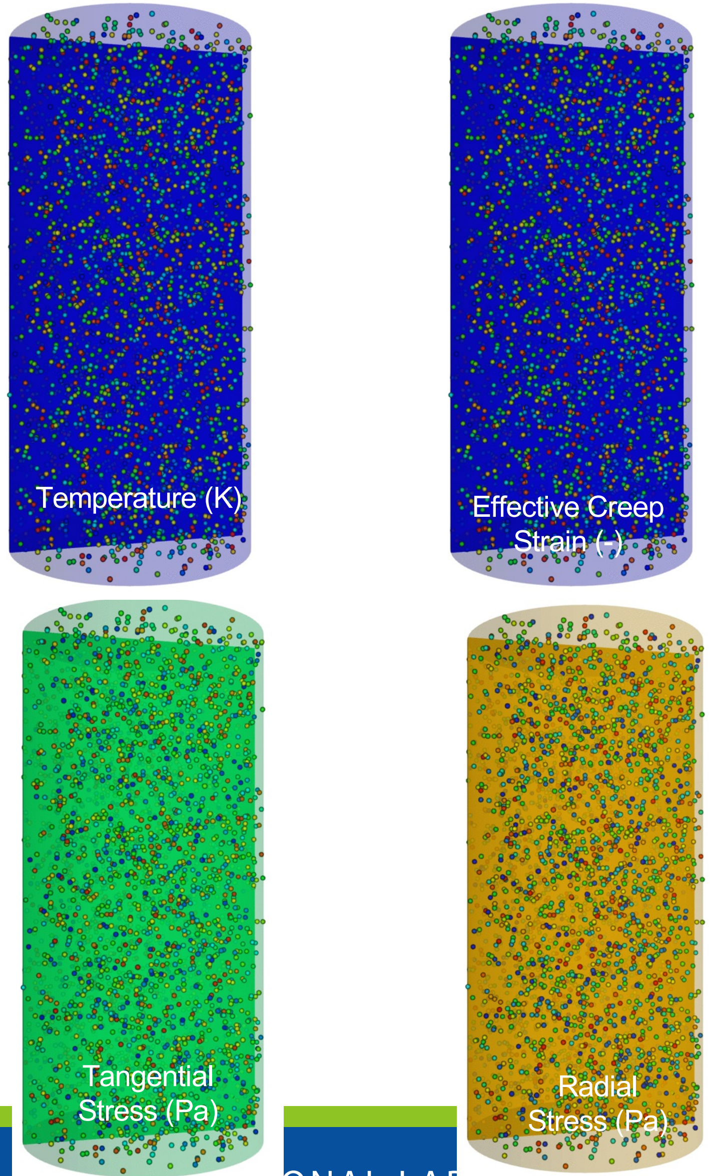

AGR-3/4

- AGR-3/4 is the combined third and fourth planned irradiations of the AGR Fuel Development and Qualification Program
- Irradiate fuel containing uranium oxycarbide (UCO) designed-to-fail (DTF) (ref kernel + PyC) fuel particles that will provide a known source of fission products for subsequent transport through compact matrix and structural graphite materials.

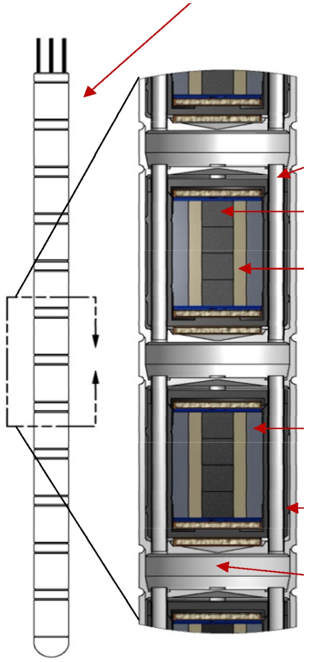

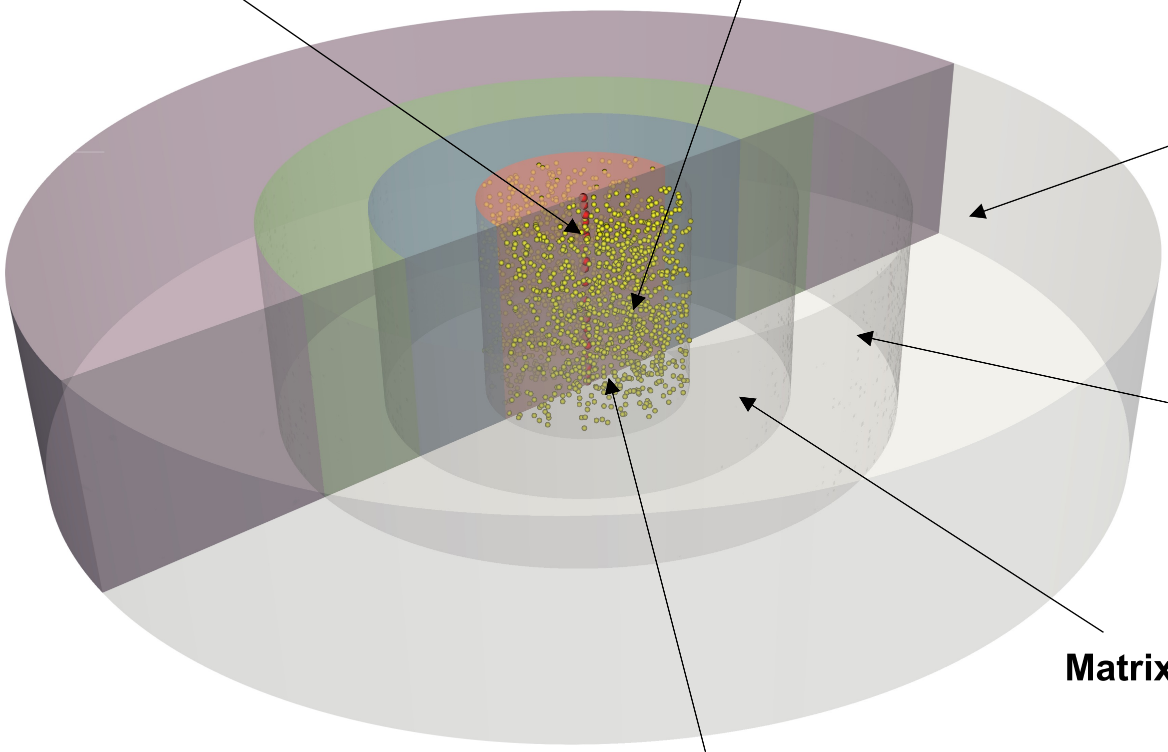

Diffusion coefficients of Matrix and Graphite

BISON solves the following heat and diffusion coupled equations:

$$\rho c_P \frac{\partial T}{\partial t} = \nabla \cdot (k \nabla T) + E_f \dot{F}$$

$$\frac{\partial C}{\partial t} + \nabla \cdot (D \nabla C) + \lambda C - p = 0$$

The diffusion coefficient is defined in Arrhenius form as:

$$D = D_0 \exp(-\frac{Q}{RT})$$

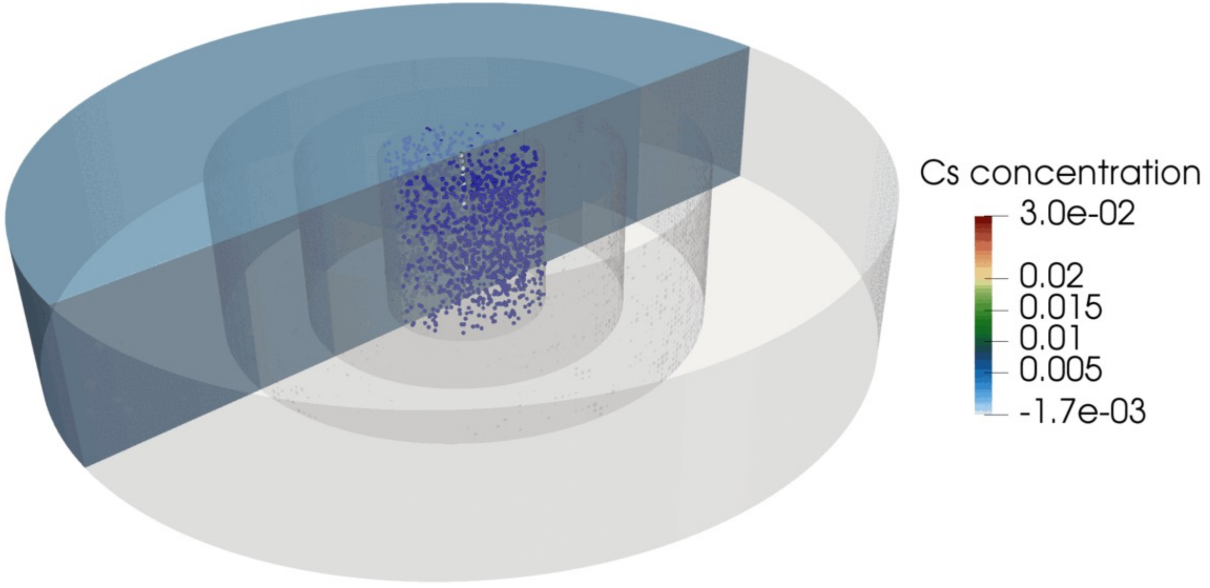

Species	Silver		Cesium		Strontium	
	D_0 (m^2/s)	Q (J/mol)	D_0 (m^2/s)	Q (J/mol)	D_0 (m^2/s)	Q (J/mol)
Matrix	1.6	258000	3.60×10^{-4}	189000	1.00×10^{-2}	303000
Graphite	1.38×10^{-2}	226000	1.70×10^{-6}	149000	1.70×10^{-2}	268000

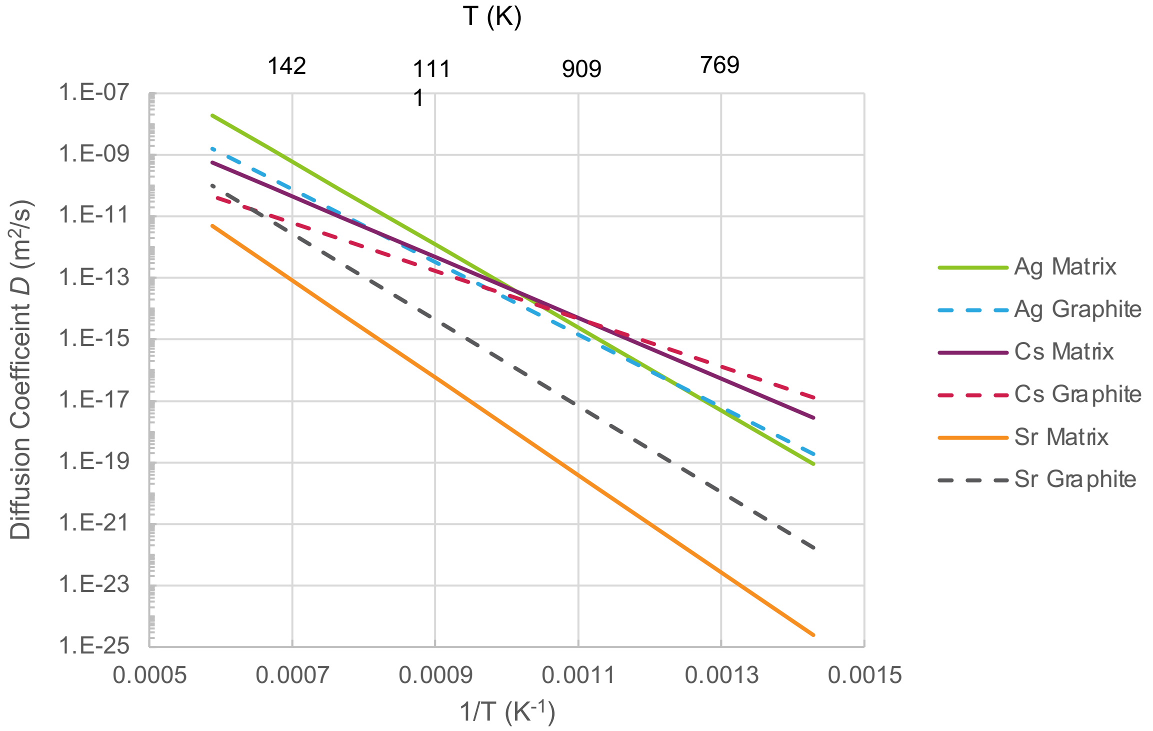

Sorption Isotherm

- The presence of gaps results in discontinuities in the fission product concentration across rings. Established sorption isotherms are used to determine the surface concentration between the two surfaces (subscripts 1 and 2) by:

$$\exp\left(A_1 + \frac{B_1}{T_1}\right) C_1^{\left(D_1 + \frac{E_1}{T_1}\right)} + \exp\left[\left(A_1 + \frac{B_1}{T_1}\right) + \left(D_1 - 1 + \frac{E_1}{T_1}\right)\left(d_{1_1} - d_{2_1} T_1\right)\right] C_1 = \exp\left(A_2 + \frac{B_2}{T_2}\right) C_2^{\left(D_2 + \frac{E_2}{T_2}\right)} + \exp\left[\left(A_2 + \frac{B_2}{T_2}\right) + \left(D_2 - 1 + \frac{E_2}{T_2}\right)\left(d_{1_2} - d_{2_2} T_2\right)\right] C_2$$

Material	Fission Product	A (-)	B (K)	D (-)	E (K)	d_1 (-)	d_2 (1/K)
Matrix	Cs	19.3	-47300	1.51	4340	3.4	6.15×10^{-4}
	Sr	54.3	-149000	-8.52	28500	3.13	0
Graphite	Cs	24.0	-35700	-1.56	6120	2.04	1.79×10^{-3}
	Sr	19.4	-40100	-0.32	4090	-2.12	0

Nominal Temp 900 C

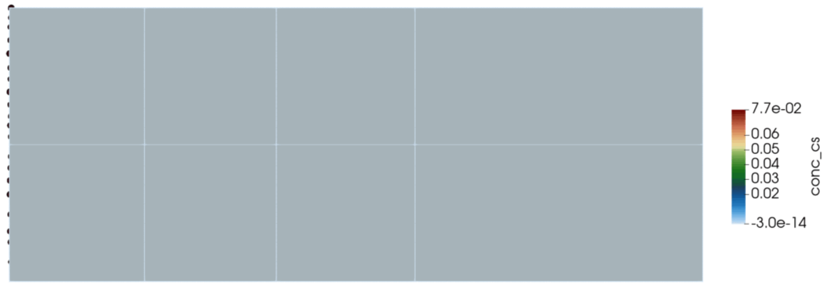

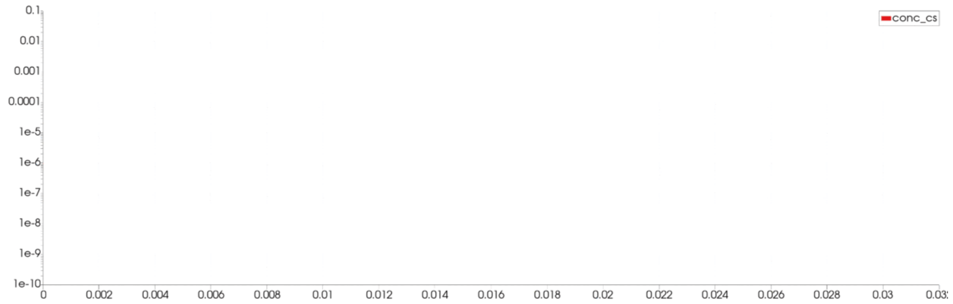

Nominal Temp 1400 C

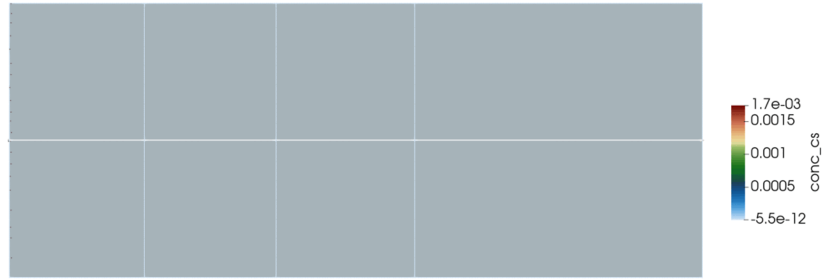

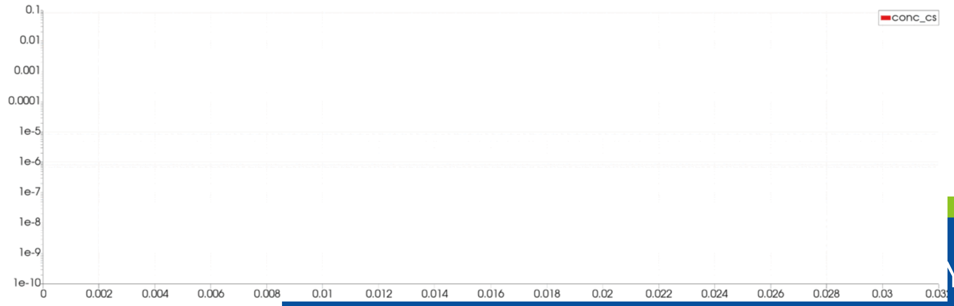

AGR-3/4 Capsule

- AGR-3/4 capsule types and ring materials

Capsule	Type	Ring Material		
		Inner	Outer	Sink
1	Std	Matrix	PCEA	PCEA
2	FB	Matrix	PCEA	PCEA
3	Std	PCEA	PCEA	PCEA
4	FB	Matrix	PCEA	PCEA
5	Std	Matrix	PCEA	PCEA
6	FB	Matrix	PCEA	PCEA
7	Std	Matrix	PCEA	PCEA
8	Std	IG-110	IG-110	PCEA
9	FB	Matrix	IG-110	PCEA
10	Std	PCEA	PCEA	PCEA
11	FB	Matrix	PCEA	PCEA
12	Std	Matrix	PCEA	PCEA

- Source terms

Capsule	Ag		Cs		Sr	
	Driver	DTF	Driver	DTF	Driver	DTF
1	0.02%	89.36%	0.00%	22.10%	0.00%	2.77%
3	23.25%	98.54%	0.00%	92.76%	0.85%	2.90%
4	3.15%	96.97%	0.00%	68.89%	0.13%	2.78%
5	4.05%	96.61%	0.00%	71.60%	0.17%	2.78%
7	64.12%	99.39%	0.20%	98.07%	4.74%	5.58%
8	3.15%	96.90%	0.00%	68.93%	0.13%	2.78%
10	32.52%	98.84%	0.01%	94.61%	1.17%	3.05%
12	0.00%	65.83%	0.00%	3.28%	0.00%	2.76%

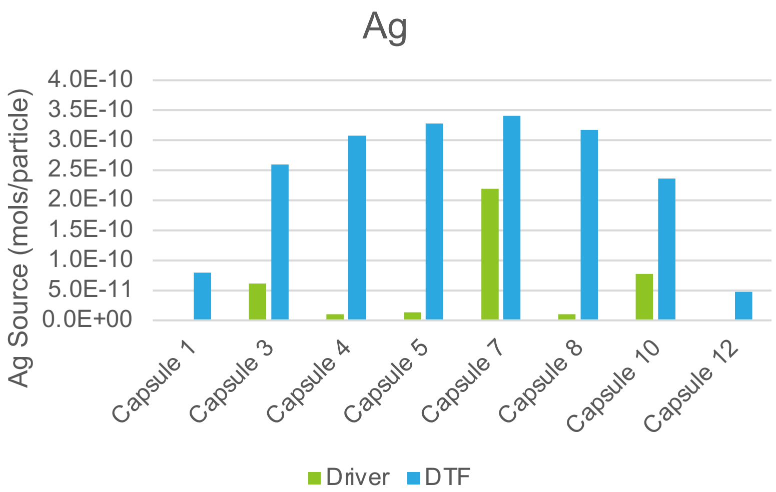

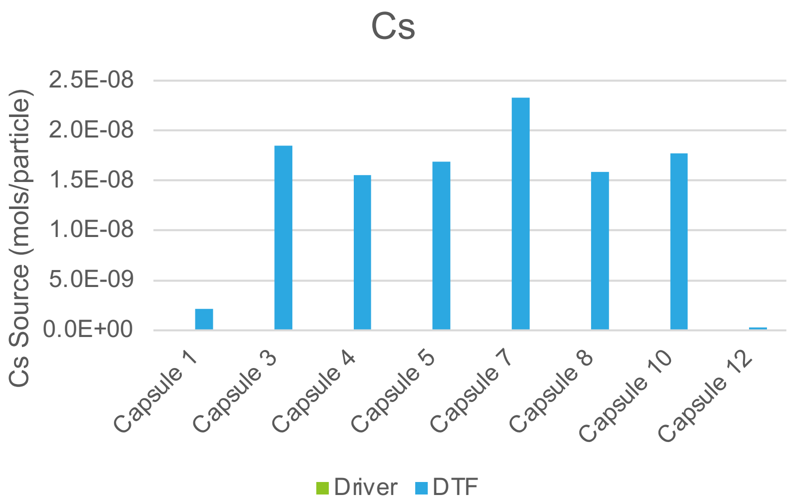

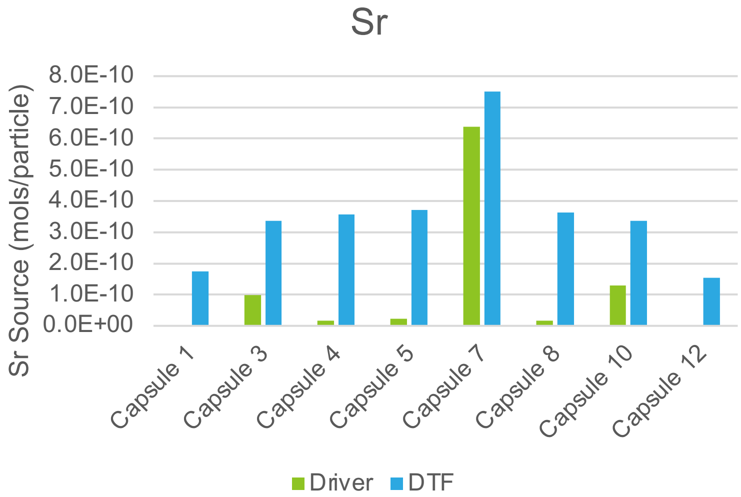

AGR-3/4 Capsule

- TAVA as-run inner and outer ring temperatures

Capsule	TAVA (°C)	Compact	Matrix		Graphite		Sink	
		Outer Temp. (°C)	Inner Temp. (°C)	Outer Temp. (°C)	Inner Temp. (°C)	Outer Temp. (°C)	Inner Temp. (°C)	Outer Temp. (°C)
12	854	849	795	771	737	731	496	486
10	1191	1159	1039	1016	975	957	665	635
8	1190	1123	1012	976	917	885	596	538
7	1345	1263	1185	1105	1028	1005	643	599
5	1015	1000	888	794	747	719	572	525
4	1008	990	901	814	771	746	609	571
3	1177	1139	1028	1004	963	952	550	519
1	927	928	874	848	757	752	511	501

- AGR-3/4 ring dimensions from PIE

Capsule	Matrix		Graphite		Sink	
	IR (mm)	OR (mm)	IR (mm)	OR (mm)	IR (mm)	OR (mm)
12	6.235	12.115	12.255	17.490	19.670	30.800
10	6.290	12.020	12.415	18.740	19.700	31.715
8	6.300	12.035	12.385	19.275	19.785	31.820
7	6.375	11.835	12.465	18.675	19.765	31.815
5	6.335	11.945	12.340	19.695	19.770	31.805
4	6.355	11.935	12.350	19.620	19.740	31.660
3	6.310	12.015	12.430	16.540	20.710	31.780
1	6.275	11.805	12.265	16.750	20.605	30.795

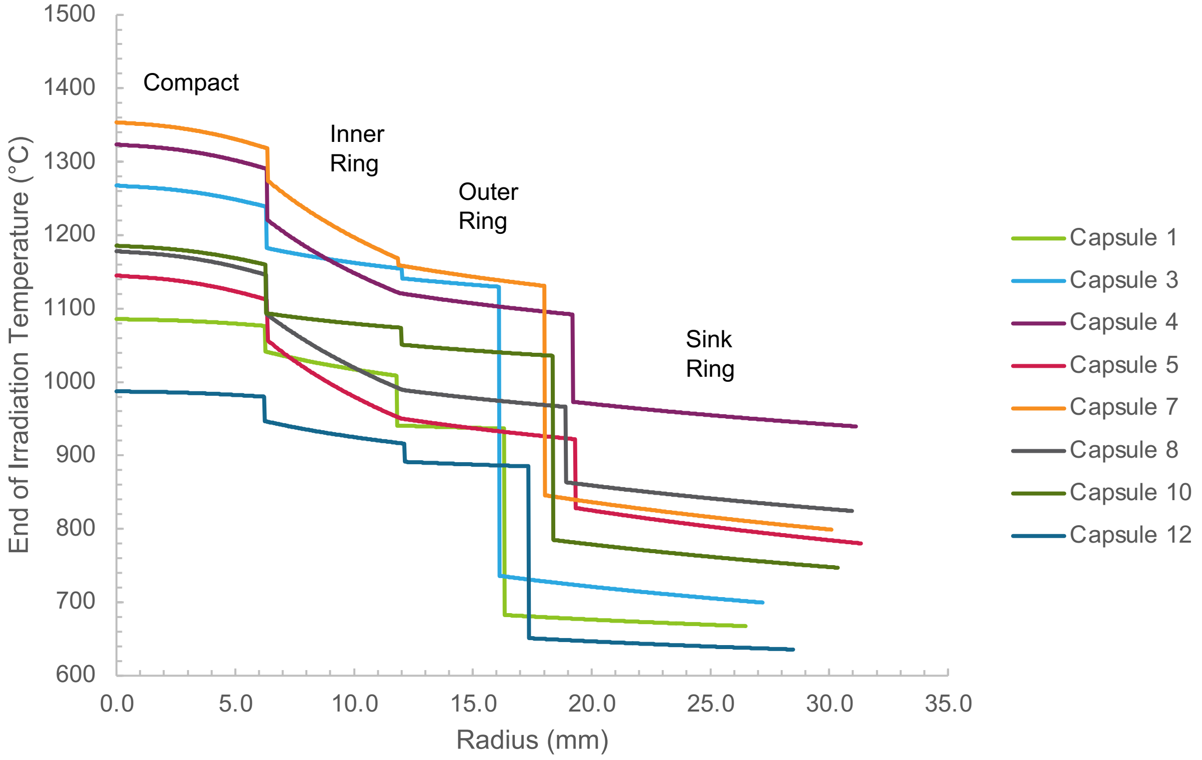

End of irradiation capsule temperature profiles calculated by BISON.

Fission Product Concentration Profiles

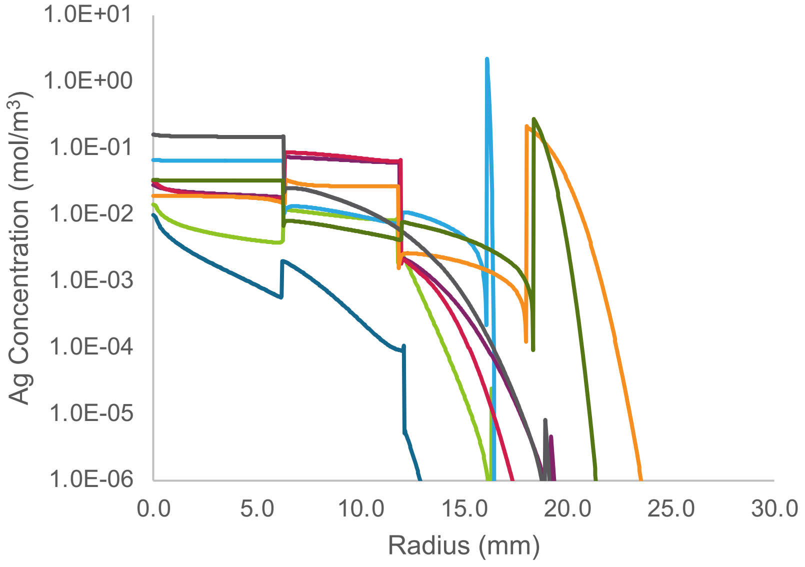

Silver concentration profiles

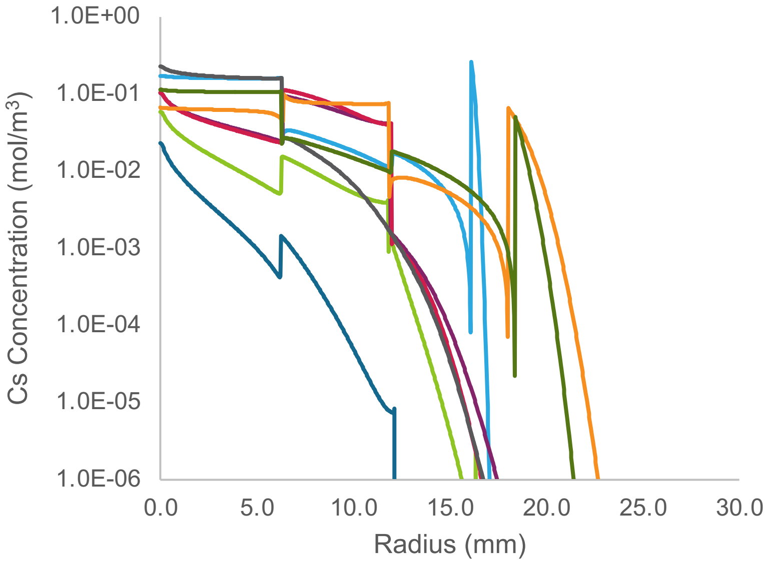

Cesium concentration profiles

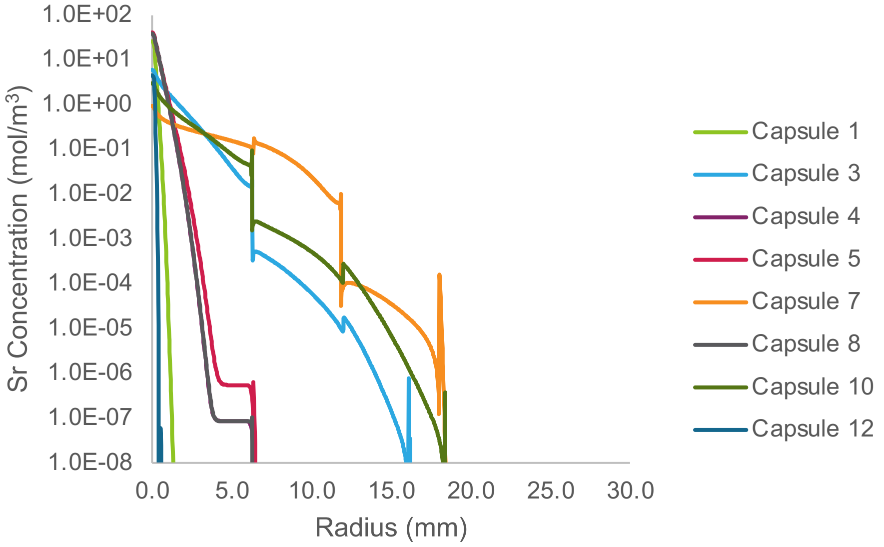

Strontium concentration profiles

Comparison to PIE Data

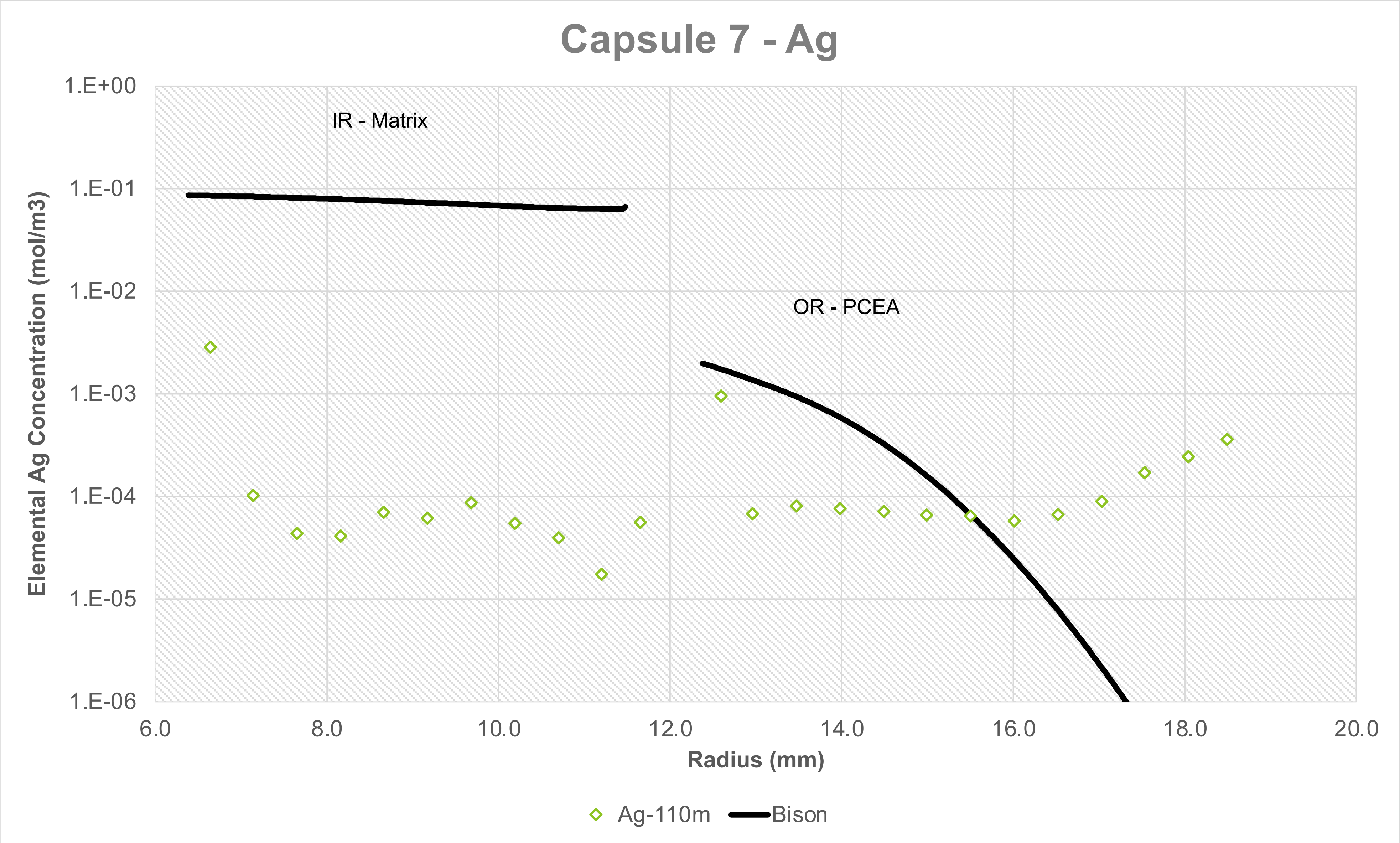

Comparison to PIE Data

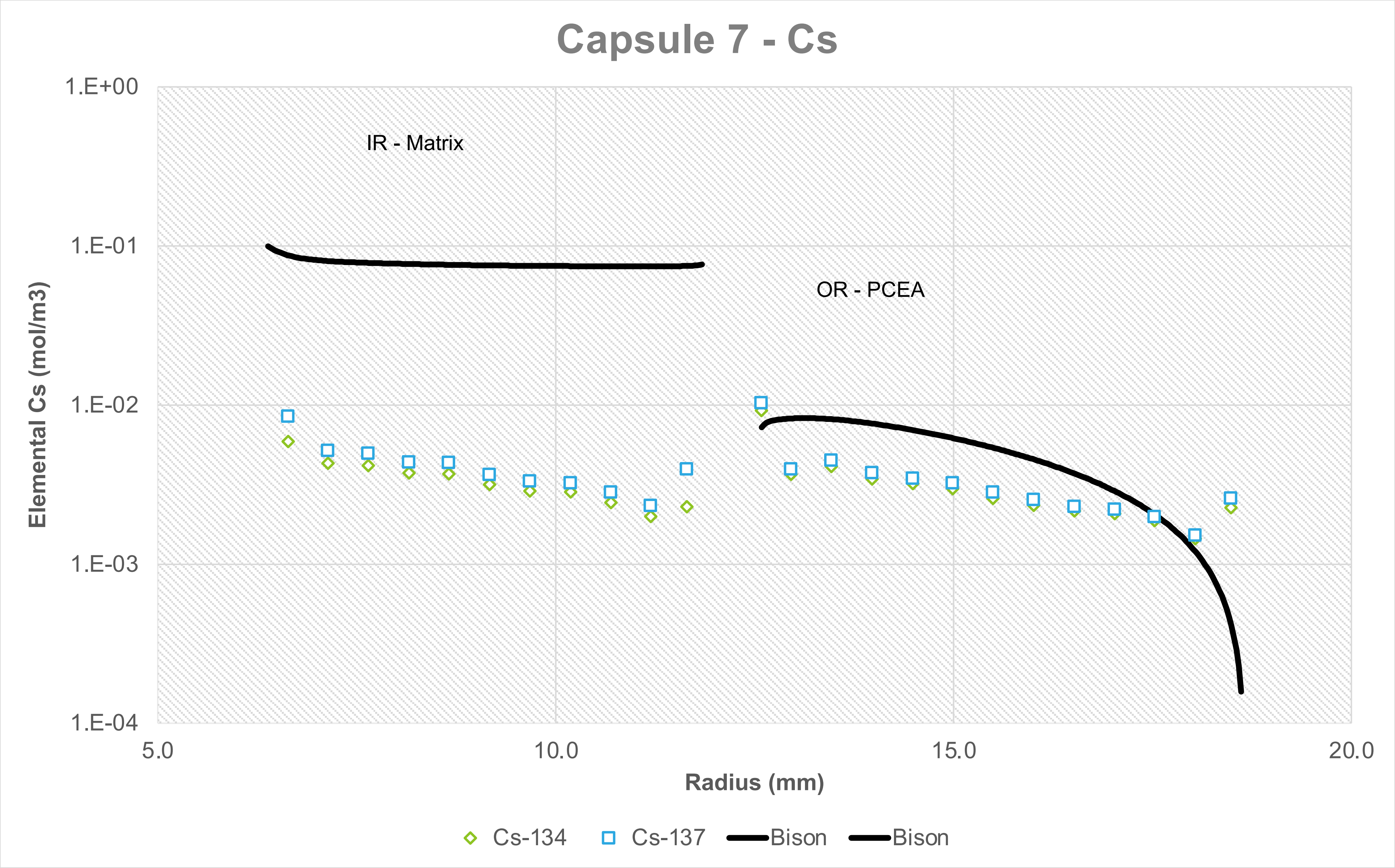

Comparison to PIE Data

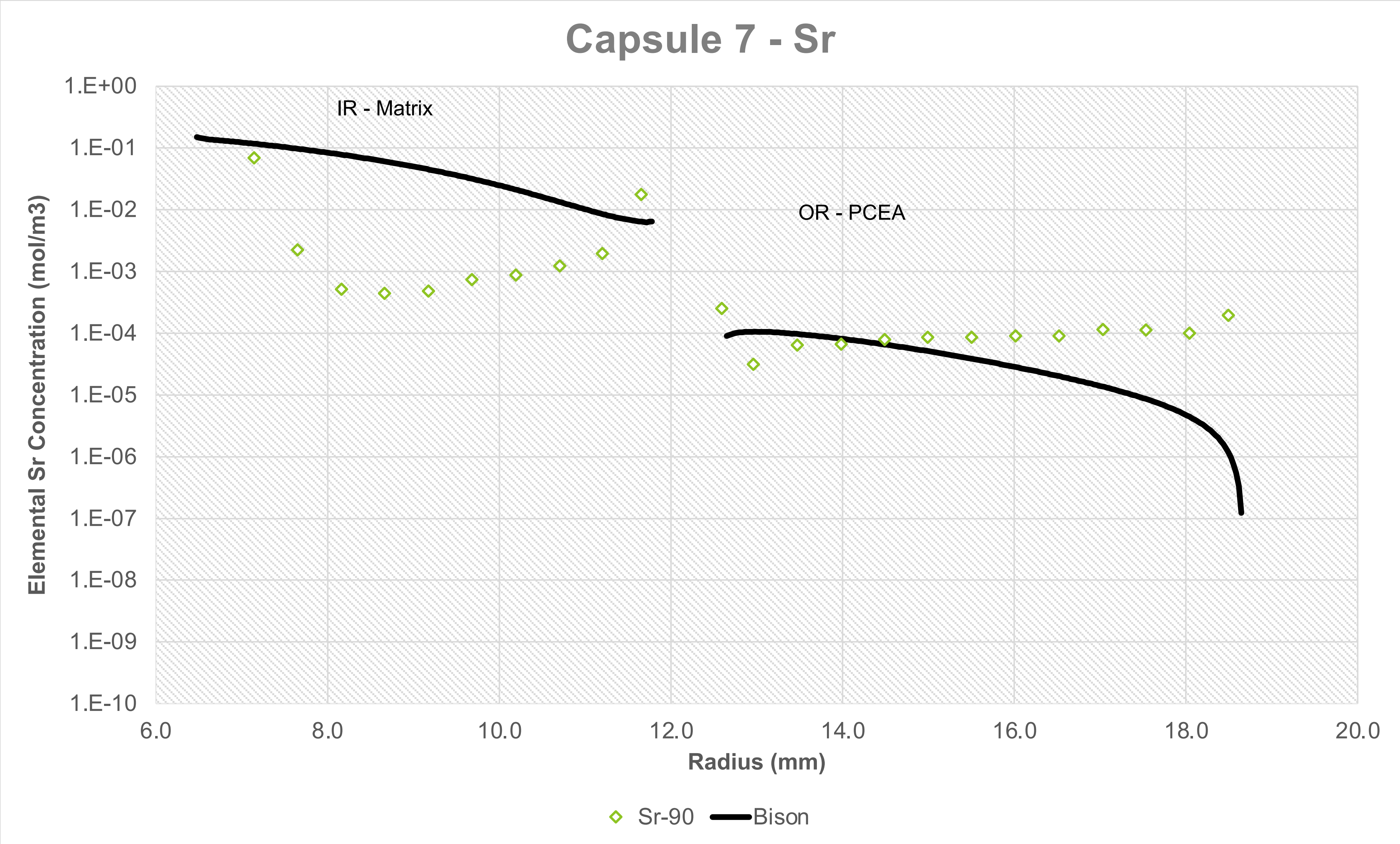

Summary

- New features in BISON to model intact/imperfect/failed particles
- Studies have highlighted the need to account for matrix retention, so new features have been developed to model entire compacts
- Mod-Exp collaboration help analyzing and understanding measurements and deriving material properties for AGR 3/4